



Completing a taxonomic puzzle: integrative review of geckos of the *Paroedura bastardi* species complex (Squamata, Gekkonidae)

Aurélien Miralles¹, Teddy Bruy¹, Angelica Crottini², Andolalao Rakotoarison³, Fanomezana M. Ratsoavina³, Mark D. Scherz⁴, Robin Schmidt⁵, Jörn Köhler⁶, Frank Glaw⁴, Miguel Vences⁵

1 Institut Systématique, Evolution, Biodiversité (ISYEB), Muséum national d'Histoire naturelle, CNRS, Sorbonne Université, EPHE, 57 rue Cuvier, CP50, 75005 Paris, France

2 CIBIO, Research Centre in Biodiversity and Genetic Resources, InBIO, Universidade do Porto, Campus Agrário de Vairão, Rua Padre Armando Quintas, N° 7, 4485-661 Vairão, Portugal

3 Zoologie et Biodiversité Animale, Université d'Antananarivo, BP 906, Antananarivo, 101 Madagascar

4 Zoologische Staatssammlung München (ZSM-SNSB), Münchhausenstraße 21, 81247 München, Germany

5 Zoological Institute, Technische Universität Braunschweig, Mendelssohnstraße 4, 38106 Braunschweig, Germany

6 Hessisches Landesmuseum Darmstadt, Friedensplatz 1, 64283 Darmstadt, Germany

<http://zoobank.org/08BE0686-2B92-461D-8BB0-592CFB025133>

Corresponding author: Aurélien Miralles (miralles.skink@gmail.com)

Academic editor Uwe Fritz | Received 25 September 2020 | Accepted 21 December 2020 | Published 26 February 2021

Citation: Miralles A, Bruy T, Crottini A, Rakotoarison A, Ratsoavina FM, Scherz MD, Schmidt R, Köhler J, Glaw F, Vences M (2021) Completing a taxonomic puzzle: integrative review of geckos of the *Paroedura bastardi* species complex (Squamata, Gekkonidae). *Vertebrate Zoology* 71: 27–48. <https://doi.org/10.3897/vz.71.e59495>

Abstract

The *Paroedura bastardi* clade, a subgroup of the Madagascan gecko genus *Paroedura*, currently comprises four nominal species: *P. bastardi*, supposedly widely distributed in southern and western Madagascar, *P. ibityensis*, a montane endemic, and *P. tanjaka* and *P. neglecta*, both restricted to the central west region of the island. Previous work has shown that *Paroedura bastardi* is a species complex with several strongly divergent mitochondrial lineages. Based on one mitochondrial and two nuclear markers, plus detailed morphological data, we undertake an integrative revision of this species complex. Using a representative sampling for seven nuclear and five mitochondrial genes we furthermore propose a phylogenetic hypothesis of relationships among the species in this clade. Our analyses reveal at least three distinct and independent evolutionary lineages currently referred to *P. bastardi*. Conclusive evidence for the species status of these lineages comes from multiple cases of syntopic occurrence without genetic admixture or morphological intermediates, suggesting reproductive isolation. We discuss the relevance of this line of evidence and the conditions under which concordant differentiation in unlinked loci under sympatry provides a powerful approach to species delimitation, and taxonomically implement our findings by (1) designating a lectotype for *Paroedura bastardi*, now restricted to the extreme South-East of Madagascar, (2) resurrecting of the binomen *Paroedura guibeae* Dixon & Kroll, 1974, which is applied to the species predominantly distributed in the South-West, and (3) describing a third species, *Paroedura rennerae* sp. nov., which has the northernmost distribution within the species complex.

Keywords

Madagascar, new species, phylogenetics, species delimitation, sympatry, taxonomy.

Introduction

The gekkonid genus *Paroedura* is endemic to Madagascar and the Comoro islands (Glaw and Vences 2007, Hawlitschek and Glaw 2013). Its monophyly has been recovered by several molecular phylogenetic studies (e.g. Jackman et al. 2008, Glaw et al. 2018). Currently, 22 species are recognized, with more than half of the species scientifically named in the course of the 21st century (Uetz et al. 2020). While some species of *Paroedura*, like for example *P. masobe* or *P. lohatsara*, can be immediately recognized by their strikingly distinct external morphology (Nussbaum and Raxworthy 1994, Glaw et al. 2001), other species are morphologically more similar to close relatives and their identification based on morphology alone remains challenging. The application of molecular genetics furthermore has revealed the existence of deep phylogenetic lineages within the genus, many of them apparently qualifying as undescribed candidate species (Jackman et al. 2008, Nagy et al. 2012, Glaw et al. 2014, 2018), indicating that the species diversity within the genus is still insufficiently documented. Integrative taxonomic approaches already helped to revise species diversity within the *P. oviceps* clade, a group of largely limestone-adapted species occurring on karstic outcrops, resulting in the description of four new species (Glaw et al. 2014, 2018). Another major clade, the *P. stumpffi* clade, has been revised by Hawlitschek and Glaw (2013) and has resulted in the discovery and description of a new species from the Comoran Island of Mayotte.

Another subgroup within *Paroedura* whose monophyly is supported by molecular data (Jackman et al. 2008, Glaw et al. 2014, 2018, Köhler et al. 2019) as well as by chromosomal data (a $2n=34$ karyotype, compared to $2n=38$ or 36 in other species of the genus, Aprea et al. 2013, Koubová et al. 2014) contains four currently recognized nominal species: *P. bastardi* (Mocquard, 1900), supposed to be widely distributed in southern and western Madagascar; *P. ibityensis* Rösler & Krüger, 1998, a montane species endemic to the region of Itremo and Ibity; and *P. tanjaka* Nussbaum & Raxworthy, 2000 and *P. neglecta* Köhler, Vences, Scherz & Glaw, 2019, both of the latter known only from the karstic Tsingy de Bemaraha formation in western Madagascar. Three recently published studies provided molecular phylogenetic trees in which the taxon *P. bastardi* was paraphyletic, with *P. ibityensis* nested among at least three strongly divergent mitochondrial lineages of *P. bastardi* and thus rendering *P. bastardi* sensu lato paraphyletic (Glaw et al. 2014, 2018, Köhler et al. 2019). The data accumulated so far strongly suggest the existence of several cryptic or morphologically similar species contained in the name *P. bastardi*, particularly as some of these divergent lineages appear to occur in sympatry at certain localities (Köhler et al. 2019). We here use the term *Paroedura bastardi* clade to refer to the entire monophyletic group of species (*P. bastardi*, *P. ibityensis*, *P. neglecta*, *P. tanjaka*) and associated putative species-level lineages, and *Paroedura bastardi* complex to refer to *P. bastardi* sensu lato, i.e., including the cryp-

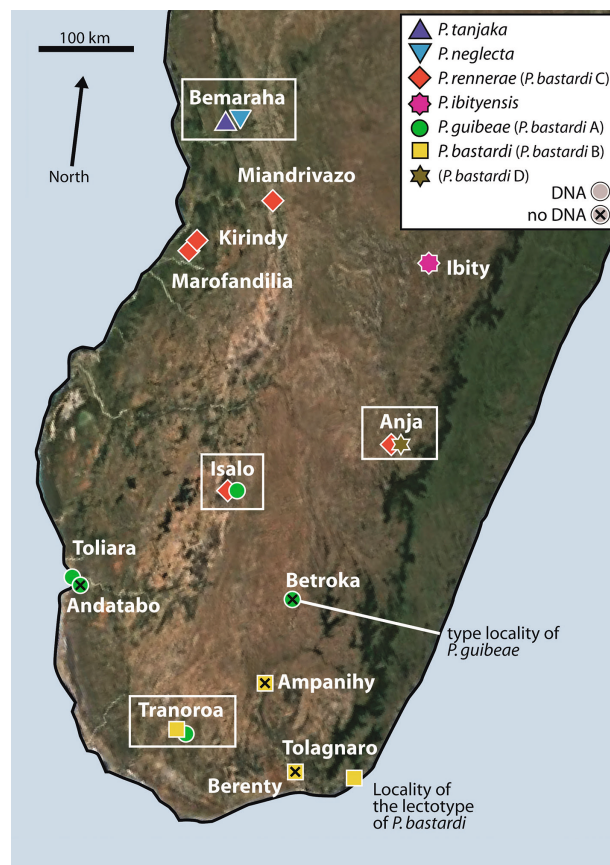


Figure 1. Localities of specimens of the *Paroedura bastardi* clade analyzed in the present study. Colored shapes represent distinct lineages (species-level taxonomic units, anticipating the results of the present study) and open white rectangles highlight co-occurrence of two lineages. Black crosses superimposed on color shapes indicate specimens for which molecular data were not available, and whose taxonomic assignment is based exclusively on morphology. The localities of Marofandilia and Miandrivazo are based on additional genetic data (two 16S sequences) from Aprea et al. (2013).

tic lineages currently associated with this species. The present work aims at elucidating species limits and thus revising the species diversity within the *P. bastardi* complex, by combining a multilocus molecular dataset (one mitochondrial and two nuclear markers) with a detailed morphological study in an integrative taxonomic framework. Furthermore, we provide a phylogenetic analysis involving a representative set of samples for an extended set of molecular markers, to infer the relationships within this clade of geckos.

Material and methods

Sampling

Geckos were collected at night by opportunistic searching in potential habitats. Voucher specimens were euthanized by injection with ketamine solution or MS-222,

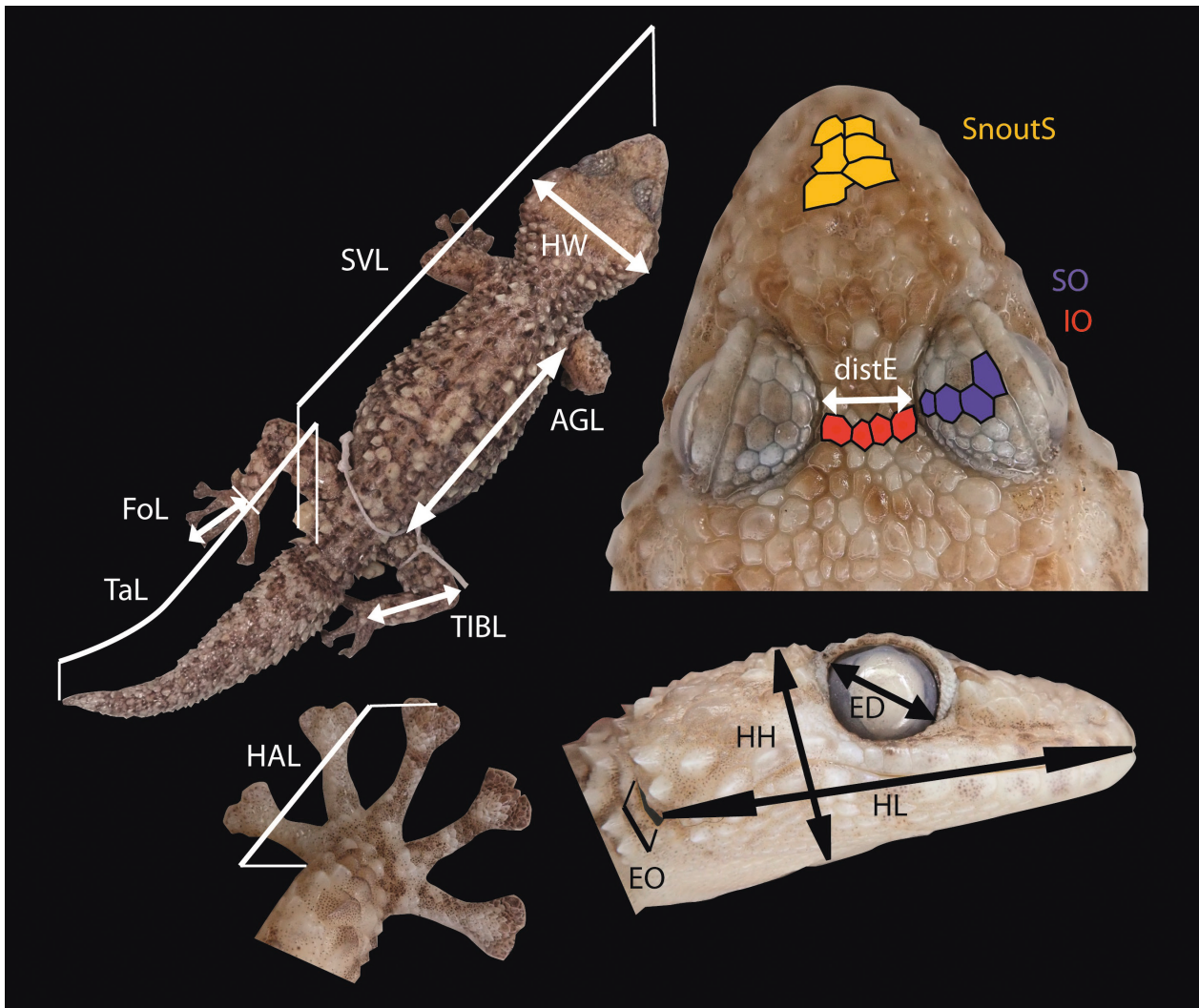


Figure 2. Illustration of the morphological characters used in this study. Quantitative characters: SVL = snout–vent length; TaL = tail length; HL = maximum head length from the anterior margin of the ear opening to the tip of the snout; HW = maximum head width; HH = maximum head height behind the eyes; distE = minimum distance between and the bony edges of the eyeballs in dorsal view; AGL = axilla–groin distance; ED = maximum eye diameter; EO = maximal ear opening; TIBL = distance between the ankle and the knee (tibia length, knee flexed at 90°, left side). Qualitative characters: IO = minimum number of interocular scales separating the eyes (above the center of the eyes); SO = number of granular scales across the upper eyelid (transversally); SnoutS = arrangement of the mediodorsal scale rows of the snout tip: mostly forming two transverse rows of granules in contact (c), separated by a third median rows (s) or intermediate pattern (i). Pictures of *P. bastardi* taken by AM.

fixed in 90% ethanol or 5% formalin, then transferred to 70% ethanol for long-term storage. Tissue samples were stored in 99% ethanol. Field numbers refer to the collections of Angelica Crottini (ACZC), Franco Andreone (FAZC), Frank Glaw and Miguel Vences (FGMV), Frank Glaw (FGZC) and Aurélien Miralles (MirZC). Vouchers were deposited in the Museo Regionale di Scienze Naturali (MRSN), the Parc Botanique et Zoologique de Tsimbazaza (PBZT), the collections of the Mention Zoologie et Biodiversité Animale of the Université d'Antananarivo (UADBA-R) and the Zoologische Staatssammlung München (ZSM). Additional specimens were examined from the collections of the Field Museum of Natural History, Chicago (FMNH), the Muséum National d'Histoire Naturelle, Paris (MNHN), the Zoological Museum Amsterdam (ZMA), and the Zoologisches Forschungsmuseum Alexander

Koenig, Bonn (ZFMK). A map showing the geographic provenance of samples examined for DNA sequences and/or morphology is represented in Figure 1. The list of specimens examined for morphology is presented in the Appendix 1.

Morphological analyses

Measurements were taken using a digital Vernier calliper to the nearest 0.1 mm (taken by TB, Fig. 2): SVL = snout–vent length; TaL = tail length; HL = maximum head length from the anterior margin of the ear opening to the tip of the snout; HW = maximum head width; HH = maximum head height behind the eyes; distE = minimum distance between the bony edges of the orbits in dorsal view; AGL = axilla–groin distance; ED = maxi-

num eye diameter; EO = maximal ear opening; FoL = foot length (from ankle to tip of the 3rd toe, left side), HAL = hand length, distance between the wrist and the tip of the longest finger (until the insertion of the claw, which is not included, left side); TIBL = distance between the ankle and the knee (tibia length, knee flexed at 90°, left side). Qualitative characters (collected by AM) are the following: IO = minimum number of interocular scales separating the eyes (above the center of the eyes); SO = number of granular scales across the upper eyelid (transversally); SnoutS = arrangement of the mediadorsal scale rows of the snout tip: mostly forming two transverse rows of granules in contact (c), separated by a third median rows (s) or intermediate pattern (i); DigC = coloration of the toes, uniform (u) or bicolor (b). Multivariate statistical analyses were performed in R 3.5.2 (R Core Team 2018) with the R studio graphic interface R studio (RStudio Team 2016). To accommodate mixed data (here, qualitative, meristic, and mensural data), we used the function PCAmix from the package PCAmixdata (Chavent et al. 2017), which combines classical principal component analysis (PCA) with multiple correspondence analysis, and the package ade4 (Dray and Dufour 2007) for visualization of principal components. Sample sizes were too small to make application of allometric growth curves for full allometry corrections, so to remove the main impact of body size on metric measurements, all measurements were size corrected by dividing them by SVL. This procedure also has the advantage of providing simple ratios that can be easily calculated from raw measurements, even in the field, and used for diagnosis if consistent interspecific differences are detected. The PCAmix function was subsequently used to normalize the dataset (centered and normed) prior to the component analyses. Specimens displaying missing data and juveniles were removed from the dataset. Analyses were performed on 22 adult or subadult specimens from both sexes with 12 quantitative and one qualitative characters (DigC was excluded from the analysis as this trait presented too many missing data).

Molecular procedures

Genomic DNA was extracted from tissue samples using proteinase K (10 mg/ml) digestion followed by a standard salt extraction protocol (Bruford et al. 1992). To delineate species, for all available tissue samples, we amplified and sequenced a DNA fragment of a mitochondrial (mtDNA) gene (cytochrome oxidase subunit 1, CO1) and fragments of two protein-coding nuclear genes (nDNA: oocyte maturation factor, CMOS; and leucine-rich repeat and WD repeat-containing protein 1239, KIAA1239). Furthermore, in order to resolve the deep phylogenetic (interspecific) relationships within the *P. bastardi* species complex, we selected seven samples representative of all species-level lineages, plus *P. picta* as out-group, and amplified and sequenced for each of them four additional fragments of mitochondrial genes: 12S rRNA (12S), 16S rRNA (16S), and NADH-dehydrogenase subunits 2 and 4 (ND2, ND4);

as well as seven additional protein-coding nuclear genes: acetylcholinergic receptor M4 (ACM4), matrix remodeling-associated protein 5 (MXRA5), phosphatidylinositol-dependent kinase 1 (PDK1), prolactin receptor (PRLR), recombination activating gene 1 (RAG1), saccin (SACS), and titin (TTN). Standard polymerase chain reactions were performed in a final volume of 12.5 µl containing 0.3 µl each of 10 pmol primer, 0.25 µl of total 10 mM dNTP (Promega), 0.1 µl of 5 U/ml GoTaq, and 2.5 µl of GoTaq Reaction Buffer (Promega). Primer sequences and PCR conditions are given in Appendix 2. PCR products were purified with ExoSAP-IT (Thermo Fisher Scientific, Waltham, MA, USA) and directly sequenced on an ABI 3130 capillary sequencer. New sequences were checked, corrected and trimmed with the software CODONCODE ALIGNER (CodonCode Corporation), and submitted to GenBank (www.ncbi.nlm.nih.gov/genbank/; accession numbers: MW311329–MW311370, MW315522–MW315525, MW318983–MW318987, MW319200–MW319361; cf. Appendix 3). Sequences were aligned using the Clustal algorithm in MEGA7 (Kumar et al. 2016).

Molecular analyses for species delimitation

To delimit species among the *P. bastardi* group, analyses based on three independent datasets and involving all the tissue samples available for specimens in the *P. bastardi* clade ($n = 57$), plus samples representing 16 different species of *Paroedura* as out-group (see details in Appendix 3A) were carried out: one phylogenetic tree was inferred based on the mitochondrial DNA dataset (mtDNA: CO1 fragment) and two haplotype networks were reconstructed based on phased nuclear loci (nDNA: CMOS and KIAA1239).

To reconstruct a phylogenetic tree from mtDNA (CO1), the best fitting substitution model was determined in MEGA 7 (Kumar et al. 2016) based on the Bayesian Information Criterion (GTR+I+G). Phylogenetic inference under the Maximum Likelihood optimality criterion was carried out, with SPR branch swapping, and the robustness of nodes was assessed with 500 bootstrap replicates, in MEGA 7 (Kumar et al. 2016).

To assess the amount of allele sharing between populations and evaluate the amount of gene flow in contact zones, we built haplotype networks using statistical parsimony, as implemented in the program TCS v.1.21 (Clement et al. 2000) implemented in PopART (<http://popart.otago.ac.nz>). We used PHASE (Stephens et al. 2001) as implemented in DnaSP v.5 (Librado and Rozas 2009) to infer haplotypes from both sets of nuclear DNA sequences (CMOS and KIAA1239), based on alignments that were trimmed to ensure that all sequences have the same length (detailed list of the haplotypes is available in the Appendix 4). Networks were imported in Adobe Illustrator to add colors (according to the corresponding mitochondrial assignment) and additional connections representing co-occurrences of different haplotypes at a given locality.

Interspecific phylogenetic relationships within the *P. bastardi* clade

In addition to the previous analyses carried out for species delimitation purposes, three complementary analyses aimed at resolving deep phylogenetic relationships among species were undertaken on a reduced sub-sample (only one specimen per delineated species of the *P. bastardi* clade) but with a significantly greater number of markers: (1) a phylogenetic analysis based on nine concatenated nuclear markers (ACM4, 380 bp; CMOS, 426 bp; KIAA1239, 869 bp; MXRA5, 795 bp; PDC, 409 bp; PRLR, 534 bp; RAG1, 1041 bp; SACS, two fragments of 975 and 1032 bp, respectively; and TTN, 849 bp); (2) an analysis based on five concatenated mitochondrial markers (12S, 1072 bp; 16S, 603 bp; ND2, 697 bp; ND4, 852 bp; and CO1, 597 bp); and (3) an analysis combining both nuclear and mitochondrial datasets (cf. Appendix 3B). These three datasets represent a total of 7310 bp, 3821 bp and 11133 bp, respectively. For most genes, the following samples were used: *P. ibityensis*, ZMA 19642 (FGMV 2002-0990); *P. neglecta*, ZSM 163/2006 (FGZC 991), *P. tanjaka*, ZSM 40/2006 (FGZC 750); and to represent the three lineages in *P. bastardi* sensu lato: ZSM 180/2004 (FGZC 332), ZSM 189/2004 (FGZC 354), and ZSM 849/2010 (ZCMV 12740). For some taxa and gene fragments, alternative samples were used, and in some cases, complemented by previously published sequences downloaded from GenBank, or in the case of the outgroup taxon *P. picta*, extracted from the full genome of this species (Hara et al. 2018). See Appendix 3B for a complete list of samples used.

Phylogenetic analyses were carried out by partitioned Bayesian Inference, using MrBayes 3.2 (Ronquist et al. 2012) with best-fit substitution models and partitions calculated using Partition Finder 2.1 (Lanfear et al. 2016) (cf. Appendix 5). For each dataset, we performed one run of 50 million generations (started on random trees) and four incrementally heated Markov chains (using default heating values) each, sampling the Markov chains at intervals of 5000 generations. The first 12.5 million generations (burn-in = 25%) were conservatively discarded and the remaining trees were retained post burn-in and summed to generate a 50% majority-rule consensus tree. For the same individual sampling we reconstructed haplotype networks for each nuclear marker, using the same methodology described in the previous section.

To compare trees obtained from mtDNA, nDNA, and the combined data sets, we calculated the *Icong* congruence index (de Vienne et al. 2007) with the *Icong* website tool (<http://max2.ese.u-psud.fr/icong/index.help.html>).

Results

Molecular analyses

Mitochondrial DNA phylogenetic tree (CO1). The deep nodes of the tree are unresolved, and the lineages con-

sidered to be part of the *Paroedura bastardi* clade are recovered as a monophyletic group with very weak support (bootstrap value = 75%). Nevertheless, three of the four nominal species currently recognized – i.e. *P. ibityensis*, *P. neglecta*, and *P. tanjaka* – are recovered as distinct and strongly supported monophyletic groups ($\geq 99\%$). Together they form an unsupported clade (36%). In contrast, *Paroedura bastardi* sensu lato is not recovered as a monophyletic unit. Instead, this nominal species is divided into four distinct deep mitochondrial lineages, hereafter referred to as *P. bastardi* A, *P. bastardi* B, *P. bastardi* C, and *P. bastardi* D (which is represented by a single individual). In the CO1 tree, these form a basal polytomy within which the *ibityensis-neglecta-tanjaka* clade is nested. Of these lineages, *P. bastardi* A corresponds to *P. bastardi* Ca02 and Ca03 of Cocca et al. (2018) and Köhler et al. (2019), while the other lineages were all referred under the name *P. bastardi* in Köhler et al. (2019). Although the relationships among these four lineages are unresolved given the lack of support, it is worth noting that *P. bastardi* C and D are topologically recovered (with no support) more closely related to the *ibityensis-neglecta-tanjaka* clade than to *P. bastardi* A and B (Fig. 3A). The respective monophyly of *P. bastardi* B and C is fully supported (100%) whereas support for the monophyly of *P. bastardi* A is very low (60%). Within *P. bastardi* A, the subclade excluding samples from Tranoroa is supported by 96%. The monophyly of *P. bastardi* D cannot be discussed further given that it is here represented by a single specimen only.

To ensure clarity and the consistency of the comparisons between the different data sets, we arbitrarily choose to use the clustering suggested by the CO1 tree as an interpretative framework, and in the following report individuals based on their mitochondrial assignment as *P. bastardi* A, B, C or D.

Nuclear DNA networks (KIAA1239 and CMOS). In terms of overall grouping of individuals, the KIAA1239 haplotype network (Fig. 3C) shows important similarities with the mtDNA tree. The specimens of each of the four main mitochondrial lineages also show closely related haplotypes in the KIAA1239 network, respectively. In each of these groups, KIAA1239 haplotypes differ most often by only one to two mutational steps (up to a maximum of five), whereas the groups are differentiated from each other by a minimum of four mutational steps (between two haplotypes of *P. bastardi* A and *P. bastardi* D) but most often by at least 10 steps. In terms of overall structuring, the only major difference between CO1 and KIAA1239 concerns the specimen ZCMV 12790 from Anja (the only representative of *P. bastardi* D in the CO1 tree), which clusters with individuals of *P. bastardi* A (Isalo, Toliara, and Tranoroa) in the KIAA1239 network.

The CMOS haplotype network (Fig. 3B) is more conserved than the KIAA1239 network (22 distinct haplotypes, versus 37 for KIAA1239). From a structural perspective, the only notable difference between the clusters suggested by the CMOS network and lineages recovered in the CO1 tree is the sharing of a haplotype between

and no voucher specimen was available for morphological comparison. Although we are confident that this clade represents a species distinct from *P. bastardi* C (no shared haplotype between these two clades co-occurring in Anja, suggesting an absence of gene flow), it is impossible, with the limited data, to determine whether this lineage is conspecific with *P. bastardi* A (affinities suggested by KIAA1239), conspecific with *P. bastardi* B (affinities suggested by CMOS), or if it represents a fourth distinct evolutionary lineage (as suggested by the CO1 tree). Further investigations, involving a larger number of samples and an examination of their morphological characteristics, are needed to clarify its status.

In previous analyses of the *P. bastardi* clade (e.g., Köhler et al. 2019), a further mitochondrial variant was included in phylogenetic trees based on CO1 sequences, i.e., the samples MRSN R3736, MRSN R3745, MRSN R2553, and FAZC 14631, all from Isalo (published by Cocca et al. 2018; GenBank accession numbers MH063359–MH063362) considered as candidate species *Paroedura bastardi* Ca01 by Cocca et al. (2018) and Köhler et al. (2019). In our study, four additional samples yielded CO1 sequences that clustered with this variant: MirZC 40, MirZC 91, MirZC 101, and MirZC 104, all from Kirindy. We have excluded all these CO1 sequences from our analysis and do not further discuss them because we are convinced they do not represent a biological entity but rather a segment of nuclear DNA of mitochondrial origin (NUMT), i.e., a nuclear pseudogene rather than a genuine CO1 sequence. This is based on four lines of evidence: (1) examination of the chromatograms of MirZC 40, MirZC 91, MirZC 101, MirZC 104 sequences identified the presence of an unambiguous stop codon; (2) sequences of three specimens (MirZC 40, MirZC 91, MirZC 104) for the 12S rRNA fragment clearly place them in the *P. bastardi* C lineage, the only lineage otherwise known from Kirindy; (3) sequences of three specimens from Isalo (MH063295: MRSN R3736; MH063296: FAZC 14631; and MH063297: MRSN R3745) for the 16S rRNA fragment unambiguously place them in the *P. bastardi* C lineage; and (4) the re-sequencing of these three specimens for the CO1 fragment (this study) confirm that the CO1 GenBank sequences MH063359–MH063362 are different and correspond to a NUMT, despite lacking stop codons.

Phylogenetic relationships of species and main lineages. Our multi-gene phylogenetic analysis included single representative samples of all nominal species of the *P. bastardi* clade, plus *P. bastardi* A, B, and C. We did not include *P. bastardi* D because we were only able to sequence two nuclear loci (out of nine) for the single sample at our disposal.

The separate analyses of concatenated nuclear versus concatenated mitochondrial datasets (nine and five markers respectively) recovered incongruent topologies ($I_{cong} = 1.14$ with $P = 0.31$, meaning that both trees are less congruent than or as congruent as expected by chance: de Vienne et al. 2007; Fig. 4). Both trees agree in placing the sympatric species *P. neglecta* and *P. tanjaka* as sister species. The mitochondrial tree places *P. ibityensis* sister to the (*P. neglecta*,

P. tanjaka) clade, and *P. bastardi* A sister to these three species, followed by *P. bastardi* C, and *P. bastardi* B. In contrast, the nuclear tree places a clade with *P. bastardi* C and *P. ibityensis* sister to the (*P. neglecta*, *P. tanjaka*) clade, and a clade with *P. bastardi* A and B sister to the remainder of species. Whereas the nuclear tree is very well supported ($PP = 1.0$ at each nodes), the mitochondrial tree is less robustly supported, with two nodes having $PP < 0.9$ (Fig. 4).

The tree involving the complete concatenated dataset (nuclear and mitochondrial) is relatively congruent with the mtDNA tree ($I_{cong} = 1.42$ with $P = 0.01$, meaning that both trees are more congruent than expected by chance), but incongruent with the nDNA tree ($I_{cong} = 1.14$ with $P = 0.31$, not more congruent than expected by chance). This suggests that the mtDNA phylogenetic signal is predominantly contributing to the topology of the combined mtDNA+nDNA tree (Fig. 4). As a main difference, in comparison with the mtDNA tree, in the combined tree the position of *P. bastardi* A and C is reversed, whereas the relationships among *P. ibityensis*, *P. neglecta*, and *P. tanjaka*, as well as the position of *P. bastardi* B as sister to all other lineages, are identical (Fig. 4).

Although this phylogeny and the underlying mitochondrial discordance remains to be confirmed by more comprehensive phylogenomic studies, it is worth noting that the suggested relationships of *P. ibityensis* with the (*P. neglecta*, *P. tanjaka*) clade coincide with the occurrence of these two groups at localities relatively distant from one another in central Madagascar: *P. ibityensis* at high elevations on rocky mountain tops in the central high plateau, and *P. neglecta* and *P. tanjaka* in the central-west (Fig. 1). The intervening area between the high plateau and the western massifs such as the Tsingy de Bemaraha is poorly studied, with few reptile records (Glaw and Vences 2007), but it is possible that these apparently related species occur in geographical proximity to one another. Also, the relationships of *P. bastardi* C with the (*P. ibityensis* (*P. neglecta*, *P. tanjaka*)) clade is biogeographically plausible as this is apparently the lineage of *P. bastardi* sensu lato that occurs furthest north (Fig. 1). The discordance might be compatible with an ancient hybridization event between the *P. bastardi* and *P. ibityensis* lineages, but such a scenario will require more extensive future investigation to ascertain.

Morphological comparisons

Within the *P. bastardi* clade, the two species *P. neglecta* and *P. tanjaka* can easily be diagnosed because both of them have the nostril in contact with the rostral scale (Köhler et al. 2019). We therefore focused our morphological comparisons on the other species and lineages, mainly relying on PCA. Raw morphological data are presented in Appendix 6 and the contributions of each variable to the first Principal Components (PCs) in Appendix 7. The three groups within the *Paroedura bastardi* complex revealed by molecular analyses (*P. bastardi* A, B, and C) were relatively well separated from each other in the first two Principal Components (PCs) of our morphol-

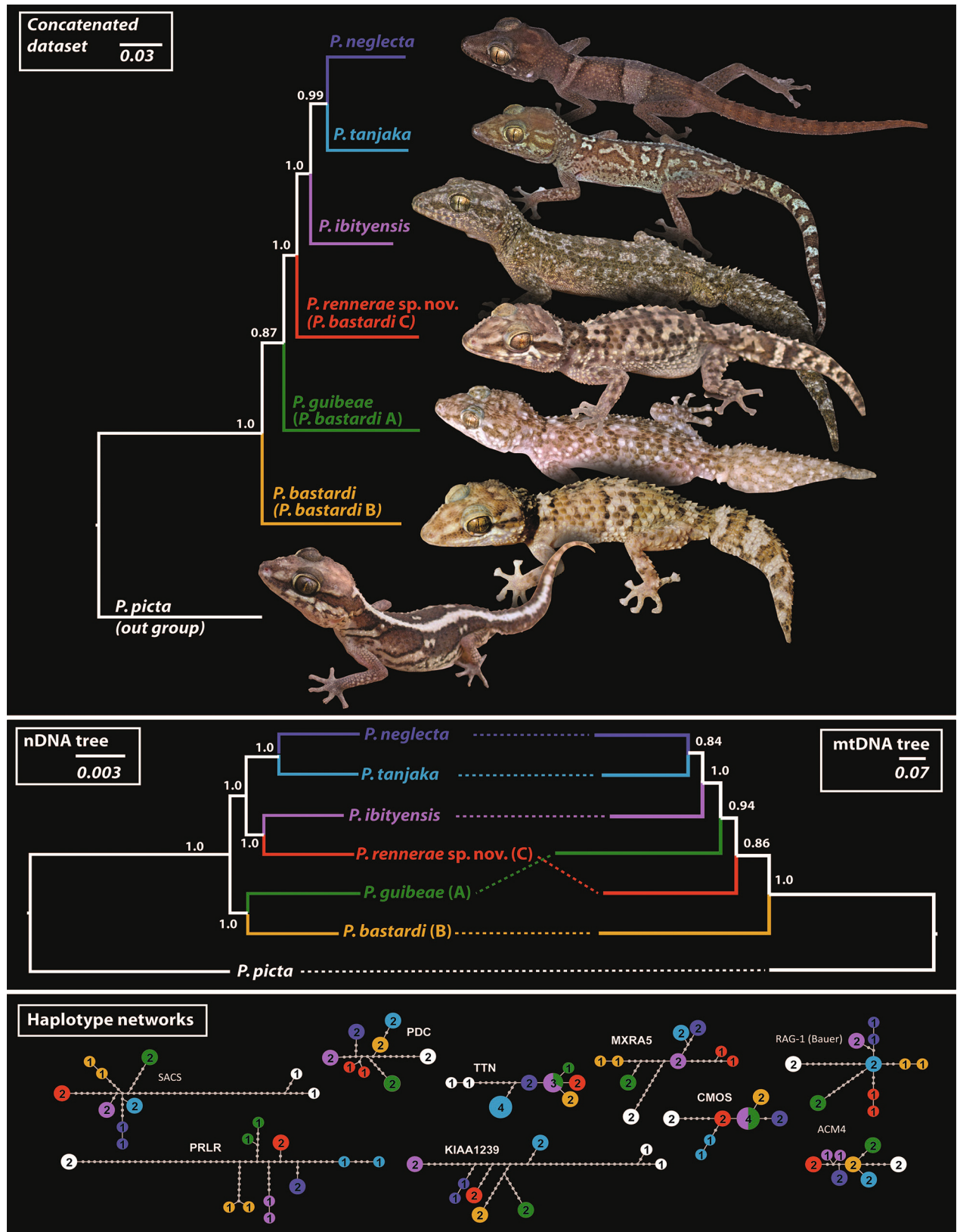


Figure 4. Multilocus phylogenetic trees (full dataset concatenated, nDNA and mtDNA concatenated trees), with haplotype networks reconstructed for each of the nuclear markers (after phasing). Photo credits: AM (*P. rennerae* sp. nov., *P. picta*, both from Kirindy), MV (*P. ibityensis* from Itremo), FG and JK (*P. neglecta* and *P. tanjaka*, both from Bemaraha), FG and MV (*P. bastardi* from Berenty, and *P. guibae* from Tranoroa).

ogy-based PCA, but poorly separated from *P. ibityensis* (Fig. 5). Relative head size (HL/SVL, HH/SVL, and HW/SVL; PC1) and body size (SVL; PC2) represent the traits

that contribute the most (> 0.50) to the variation expressed along the first two PCs. Nevertheless, although the different values related to head shape (HL/SVL, HH/SVL and

HW/SVL) contribute, along with body size, to unambiguously differentiate few pairs of species in the PCA (i.e., no overlap in the two-dimensional space of PC1 and PC2 comparing *P. bastardi* B and C with *P. bastardi* A), neither of these single variables is unambiguously diagnostic for any species. For instance, *P. bastardi* B and C reach larger body sizes than *P. bastardi* A and *P. ibityensis* (Fig. 5B), but with considerable overlap. Relative head length (HL/SVL) in *P. bastardi* B is > 0.3 for all nine adult and subadult individuals measured (0.302–0.336) and < 0.3 in *P. bastardi* A for five out of eight individuals measured (0.289–0.299); however, three *P. bastardi* A have values in the range of *P. bastardi* B (0.307–0.322) (see Appendix 7 for measurements and ratios of all individuals). Therefore, the value of these ratios for reliable, practical field identification of specimens is limited, although some statistical differences appear to exist and we expect relative head size having higher discriminatory power when comparing lineages of the *P. bastardi* complex with several other *Paroedura* species.

Integrative species delimitation: Molecular evidence of reproductive isolation in contact zones

While *P. ibityensis* is a highland species apparently not occurring in sympatry with any other lineage of the *P. bastardi* clade, among the other lineages there are several instances of co-occurrence without genetic admixture that are informative to infer reproductive isolation, as examined in the following.

(1) Sympatry in Isalo. Several specimens from Isalo are placed in *P. bastardi* A (ACZC 1828, 6464, 7932, and 7934, plus MH063363–69 available on GenBank) in the mitochondrial (CO1) tree, and those sequenced for the nuclear genes consistently show affinities to other *P. bastardi* A specimens (from Toliara and Tranoroa) in the KIAA1239 and CMOS haplotype networks. In contrast, three other specimens from Isalo are placed in *P. bastardi* C (ACZC 6438, 6534, and 7938) in the CO1 tree and consistently show affinities to other *P. bastardi* C specimens (from Kirindy and Anja) in the KIAA1239 and CMOS networks.

(2) Sympatry in Tranoroa. Three specimens of *P. bastardi* A in the CO1 tree (FGZC 352, 353, and 354) present affinities to other samples of this lineage in the KIAA1239 network, whereas in the CMOS network, they share a haplotype with specimens of *P. ibityensis*. In contrast, two other individuals of Tranoroa placed in the *P. bastardi* B clade in the CO1 tree (FGZC 332 and 327) have their nuclear haplotypes consistently recovered as closely related (or identical) to those of other *P. bastardi* B specimens (from Tolagnaro).

(3) Sympatry in Anja. Haplotypes of two specimens placed in *P. bastardi* C in the CO1 tree (ZCMV 12789 and 12791) consistently show affinities to other specimens of *P. bastardi* C (from Kirindy and Isalo) in both

the KIAA1239 and CMOS networks. In contrast, the only representative of *P. bastardi* D (ZCMV 12790), shows either affinities to specimens of *P. bastardi* A (KIAA1239 network) or to *P. bastardi* B (CMOS network).

(4) Sympatry in Bemaraha. *Paroedura neglecta* and *P. tanjaka* are sympatric in this locality. Both species represent distinct mtDNA lineages and do not share any nuclear haplotypes (CMOS, KIAA1239).

Such patterns, consistently involving the same clusters of specimens for each of the three sequenced markers, strongly support the hypothesis of at least four occurrences of sympatry with reproductive isolation between different pairs of lineages. To summarize, our dataset supports reproductive isolation between: *P. bastardi* A and C in Isalo, *P. bastardi* A and B in Tranoroa, *P. bastardi* C and D in Anja, and between *Paroedura neglecta* and *P. tanjaka* in Bemaraha (Fig. 3).

Integrative species delimitation: Morphological divergence in contact zones

The molecular evidence for reproductive isolation between different pairs of sympatric lineages of the *P. bastardi* complex in Anja, Isalo, and Tranoroa also offers an opportunity to understand more precisely the morphological variability encountered, by differentiating the features whose variability is due to intraspecific polymorphism within the same species (and which are most often variable across the distribution range), from those which characterize each of the considered species. The distinction between these two cases of polymorphism (intra- versus interspecific) could even be facilitated if the interspecific morphological differentiation has been exacerbated in sympatry by reinforcement mechanisms (i.e. character displacement). Unfortunately, the heterogeneity of the material at our disposal, and the lack of multiple adult individuals, did not always allow us to objectively link molecular and phenotypic data. For instance, for Anja, we had only two voucher specimens available for morphological examination (ZSM 850/2010, member of the clade C, and ZSM 779/2009, also a member of the clade C, but a subadult; 16S sequence available in GenBank confirm species identity: MT981881); and for Isalo, we had only one voucher specimen available (ZFMK 59808), too old to be genotyped using classical PCR approaches.

Luckily, our sampling from the population of Tranoroa was richer and provided us with several specimens unambiguously belonging to each of the two co-occurring lineages: three genotyped vouchers of *P. bastardi* A (an adult, ZSM 189/2004; a subadult, ZSM 187/2004; and a juvenile, ZSM 188/2004) and two genotyped vouchers of *P. bastardi* B (a juvenile, ZSM 178/2004; and an adult, ZSM 180/2004).

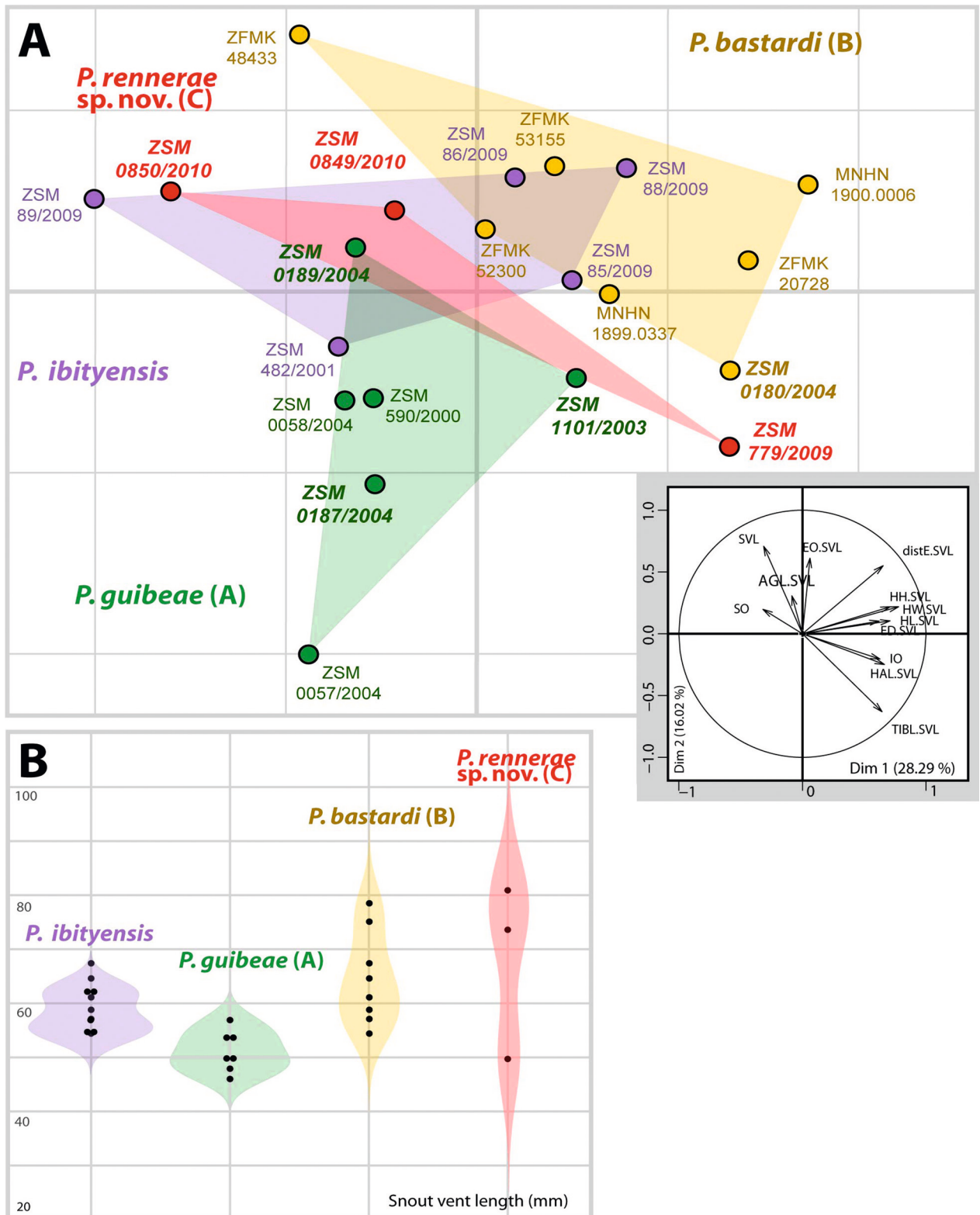


Figure 5. Morphological differentiation among four lineages of the *Paroedura bastardi* clade, here considered as representing distinct species. **A** Scatterplot of first two principal components (PC1, PC2) from a Principal Component Analysis using the morphological variables (adults and subadults only, males and females not analysed separately). Genotyped specimens are highlighted in bold italics (other specimens tentatively assigned to one of the molecular clusters based on morphological examination). **B** Violin plot of SVL (in mm), illustrating lower maximum body sizes in *P. ibityensis* and especially, in *P. guibeeae* despite overlap of size ranges among all lineages. See appendices 6 and 7 for details.

Adults and subadult specimens in Tranoroa. Despite the limited sample size and lack of molecular assignment of one specimen (ZSM 58/2004), morphological quali-

tative examinations and multivariate statistical analyses appear to confirm the morphological differentiation between the two lineages occurring in this locality. Spec-

imens of *P. bastardi* A are indeed smaller in size than those of *P. bastardi* B, have fewer interocular scales (3 to 4 versus 5 to 6); and visually differ by less prominent tubercles, by a paler coloration, and by the presence of a banded pattern with alternating dark and light stripes on fingers and toes (versus a darker coloration, more spiny tubercles and a uniform light coloration of digits in *P. bastardi* B; Fig. 6A).

Juvenile specimens in Tranoroa. Juvenile coloration can be informative in lizard taxonomy, as their patterns tends to be more pronounced (more contrasted and differentiated) than in adults, and especially in *Paroedura*, juveniles often have a distinct and species-specific color pattern. For instance, Glaw et al. (2001) emphasized the distinct juvenile coloration of *P. lohatsara*, and Köhler et al. (2019) used the unique number of dorsal bands in juvenile *P. neglecta* in the diagnosis of this species from other *Paroedura* not belonging to the *P. bastardi* clade. It is nevertheless important to take into consideration the fact that in *Paroedura*, the coloration intensity changes dramatically (and thus likely rapidly) during ontogeny. Differences between juveniles in color and pattern should therefore be interpreted with great caution, as it can be difficult to distinguish ontogenetic from inter-individual or inter-specific variation. We had the opportunity to examine two juvenile specimens of approximately identical size, and therefore supposedly at relatively similar developmental stages, from Tranoroa (Fig. 6B; ZSM 178/2004, genetically assigned to *P. bastardi* B, SVL = 30.0 mm, and ZSM 188/2004, genetically assigned to *P. bastardi* A, SVL = 26.4 mm). The latter specimen (cluster A) has a dull dorsal coloration whereas the former specimen (cluster B) shows a highly contrasted color pattern consisting of a dark brown dorsal background with two very light transverse bands. This pattern is also observed in five other juveniles of similar size: ZSM 42/2004 from Tolagnaro; one syntype of *P. bastardi*, MNHN 1899.0338, from Tolagnaro; and ZFMK 48434–48436, all from Berenty), all from a part of Madagascar where only the presence of *P. bastardi* B has been confirmed by molecular data. These six juvenile specimens (the one from Tranoroa and the five others from the region of Tolagnaro) also share a similar pattern in the parietal region, which roughly evokes a butterfly or a bat-like silhouette perforated in its center (Fig. 6B, 6C). The shape of this pattern is remarkably constant across these six specimens and seems to characterize the juveniles of *P. bastardi* B.

Taxonomic conclusions

The three molecular datasets (Fig. 3) consistently suggest that *Paroedura bastardi* A, B, and C represent independent and reproductively isolated evolutionary lineages, i.e., distinct biological species, whereas the status of *Paroedura bastardi* D remains to be assessed in the future. This conclusion is supported by morphological data, despite limited genotyped material available for examination. From a nomenclatural point of view, two

taxon names unambiguously referring to populations of the *Paroedura bastardi* complex are available:

(1) *Phyllodactylus bastardi* Mocquard, 1900, whose type series is composed of five syntypes: three females (including two subadults) collected by Grandidier (MNHN 1899.0337, “environs de Tuléar” (= vicinity of Toliara) and MNHN 1899.0338 and 1899.0339, both from “Fort-Dauphin” (= Tolagnaro), and two specimens collected by M. Bastard (MNHN 1900.0006 and 1900.0007, both from the “pays Mahafaly” (= Mahafaly country), which were larger in size and darker in coloration at the time the species was named (according to Mocquard 1900). In all likelihood, this type series is mixing different clades: MNHN 1899.0337 is likely a member of *P. bastardi* A, the only lineage of the *P. bastardi* complex known to be present in Toliara, and MNHN 1899.0338 and 1899.0339 are very likely members of *P. bastardi* B, the only lineage of the *P. bastardi* complex known from Tolagnaro. Although the PCA shows morphological resemblances between the specimen MNHN 1900.0006 and those assigned to *P. bastardi* B, we consider that reliable assignment of MNHN 1900.0006 and 1900.0007 to a given genetic lineage based on morphology alone is not possible because the “Pays Mahafaly” designates a vast region of the South of Madagascar where we suspect several lineages occur.

We therefore elect to designate the syntype MNHN 1899.0338 (see Fig. 6C and Fig. 7 for photos of the head and the entire body, respectively) from Tolagnaro as lectotype of the name *Phyllodactylus bastardi* Mocquard, 1900. Although this specimen is a juvenile, we consider it the best choice because (1) all the genotyped specimens from this locality are unambiguously assigned to *P. bastardi* B, (2) this specimen presents the typical “butterfly-shaped” pattern (albeit discolored and hardly visible) observed in another juvenile unambiguously genetically assigned to *P. bastardi* B (ZSM 178/2004, Tranoroa) and in all other juveniles (not genotyped) from the extreme South East of Madagascar (ZSM 42/2004 from Tolagnaro, ZFMK 48434–48436 from Berenty) where only *P. bastardi* B is known to occur (Fig. 6B, 6C). The choice of this lectotype is also motivated by our aim to promote nomenclatural stability, by limiting the establishment of new names (it enables us to erect one of the former synonyms, *guibae*, for *P. bastardi* A, rather than erecting a new name; see below). As a consequence of our lectotype designation, the name *Paroedura bastardi* (Mocquard, 1900) becomes restricted to the specimens corresponding to *P. bastardi* B (= *Paroedura bastardi* sensu novo), and four of the original syntypes (i.e. MNHN 1899.0337, 1899.0339, 1900.0006, and 1900.0007) lose their status of name-bearers and become paralectotypes.

(2) *Paroedura guibae* Dixon & Kroll, 1974, whose holotype is an adult male (FMNH 73049) collected at “10 km S Betroka 23° 18' S 46° 06' E, Madagascar”. This *nomen* has been synonymized with *P. bastardi* by Nussbaum and Raxworthy (2000). We consider that FMNH 73049 very likely belongs to *P. bastardi* A because it

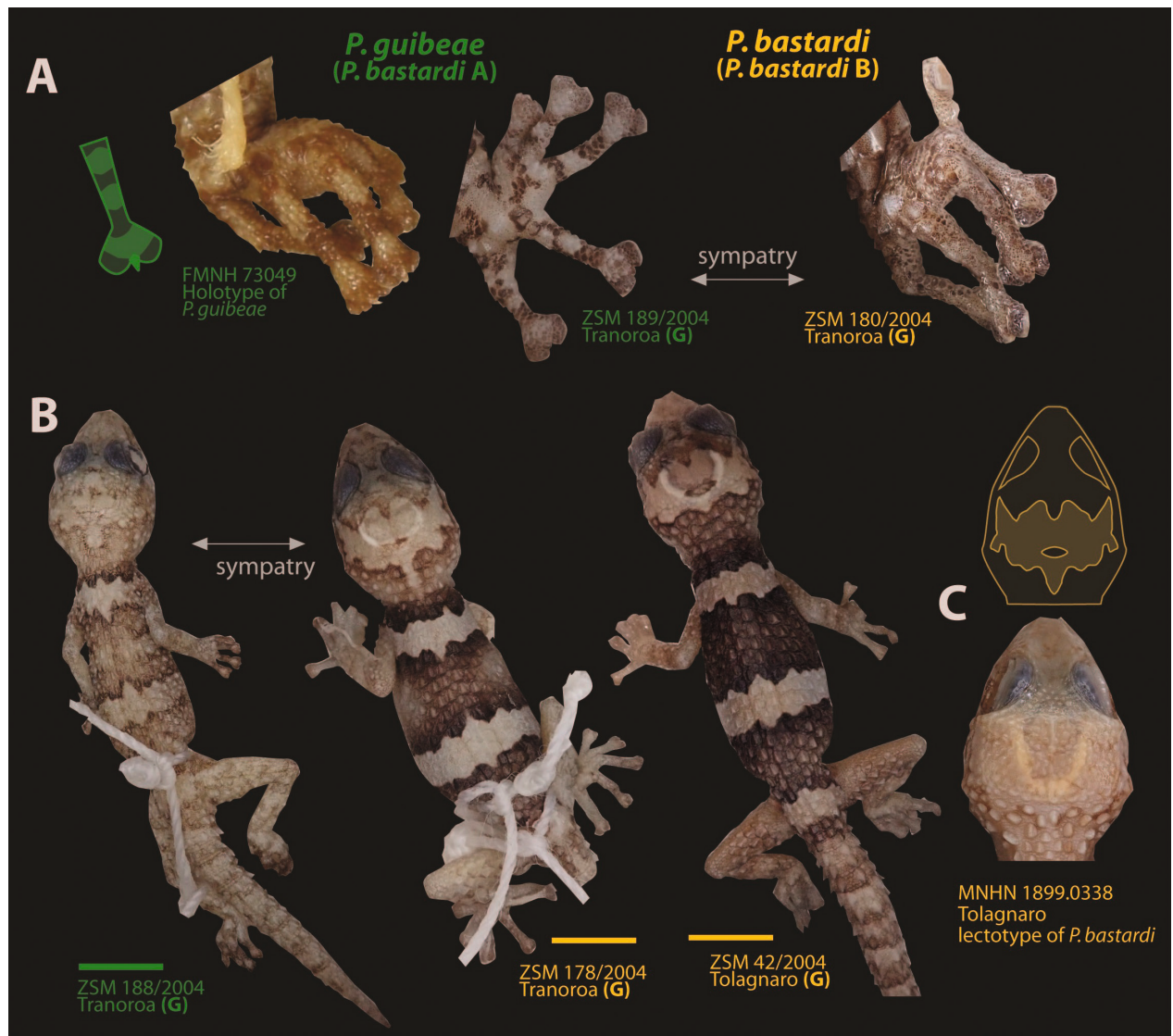


Figure 6. Differences in coloration between juveniles of lineages provisionally named *P. bastardi* A and *P. bastardi* B (corresponding to the species *P. guibeeae* and *P. bastardi*, according to the taxonomic hypothesis proposed herein), with a special emphasis on those from Tranoroa. **A** Digit coloration. Juveniles of *P. bastardi* A present a very characteristic banded pattern on fingers and toes (finger schematically represented in green). The same pattern is also present in the holotype of *P. guibeeae*, and this name is therefore assigned to *P. bastardi* A. **B** Juvenile of *P. bastardi* A showing a dull dorsal coloration, whereas the juveniles of *P. bastardi* B show a highly contrasted pattern color consisting in a dark brown dorsal background with two very light transverse bands. **C** Detail of the dorsal side of the head of the newly designated lectotype of *P. bastardi* (above, a schematic drawing represent the “butterfly” pattern characterising juveniles of *P. bastardi* B, which is also present, although hardly distinguishable (probably faded) in the lectotype of *P. bastardi*). Scale bars = 5 mm. Genotyped specimens are marked by the letter (G). Photo credits: FMNH 73049 ©Field Museum of Natural History. Created by Field Museum of Natural History, Amphibian and Reptile Collection and licensed under CC-BY-SA 4.0; all other pictures taken by AM.

shows banded patterns on digits, a trait that characterizes most of the specimens assigned to this lineage and that is always absent in the specimens assigned to *P. bastardi* B and C (cf. Fig. 6A). As a consequence, we here resurrect the name *Paroedura guibeeae* Dixon & Kroll, 1974 and unambiguously apply it to *P. bastardi* A.

Note: The spelling of the epithet of *Paroedura guibeeae* Dixon & Kroll, 1974 has been subsequently changed into *guibei* by Michels and Bauer (2004), who supported this decision by the fact that this species was originally dedicated to Mr. (not Ms.) Jean Guibé. Nevertheless, from a

nomenclatural perspective, this emendation of epithet is incorrect (unjustified emendation according to the articles 33.2 and 33.4 (ICZN 1999); see also Dubois 2007 for this particular case) and for this reason we retain the original spelling.

No earlier name is available for the species corresponding to *P. bastardi* C, and consequently, this lineage is, in the following, described as a new species.

Paroedura rennerae sp. nov.

<http://zoobank.org/545AB313-3821-414F-9A26-FFFD3B257BB>
Figs. 4, 7–9

Remarks. This species was previously named *P. sp. aff. bastardi* Ca01 “Marofandilia/Miandrivazo” by Cocca et al. (2018) and *Paroedura bastardi* by Aprea et al. (2013) and Köhler et al. (2019; partim).

Holotype. ZSM 849/2010 (ZCMV 12740), adult female, from Kirindy reserve CNFEREF, Camp de base, 20.0674°S, 44.6569°E, ca. 55 m above sea level, Atsimo-Andrefana Region, western Madagascar, collected on 2 December 2010 by A. Miralles and A. Rakotoarison.

Paratypes ($n=2$). ZSM 779/2009 (ZCMV 13023), subadult specimen of unknown sex, from Ambalavao, Anja reserve, 21.8522°S, 46.8443°E, 972 m a.s.l., Haute Matsiatra Region, Madagascar, collected on 08 December 2009 by A. Crottini, D.J. Harris, I.A. Irisarri, A. Lima, S. Rasamison, and E. Rajeriarison; and ZSM 850/2010 (ZCMV 12791), adult specimen from Anja reserve, 21.8519°S, 46.8440°E, Haute Matsiatra Region, Madagascar, collected on 08 December 2010 by A. Miralles and F. M. Ratsoaovina.

Additional non-type material. ZFMK 59808, juvenile (but not neonate) specimen from Isalo. Two specimens deposited at the University of Antananarivo (field numbers ZCMV 12789 and 12790, not presently examined), collected on 08 December 2010 by A. Miralles and F. M. Ratsoaovina, both from Anja reserve, 21.8519°S, 46.8440°E, Haute Matsiatra Region, Madagascar.

Diagnosis. *Paroedura rennerae* sp. nov. is characterized by the unique combination of the following characters: (1) presence of prominent dorsal tubercles arranged in regular longitudinal rows, (2) presence of three broad light crossbands on the dorsum in juveniles and subadults, (3) spines on the tail, (4) nostril separated from rostral scale by prenasal, and (5) a curly-bracket shaped marking in the occipital region.

Paroedura rennerae sp. nov. can be distinguished from most other currently recognized *Paroedura* species by the presence of only three broad light crossbands on the dorsum in juveniles and subadults (the first one between forelimbs, the second one at midbody, and the third one between hindlimbs) versus four light crossbands in all other species except those of the *P. bastardi* clade (*P. bastardi*, *P. guibeae*, *P. ibityensis*, *P. neglecta*, and *P. tanjaka*, which all have three crossbands) and *P. oviceps* and *P. vahiny* (in which the juvenile coloration is still unknown). It can be distinguished from *P. gracilis* by larger dorsal scales, absence of a white tip to the original tail, absence of a raised vertebral ridge on the dorsum and shorter forelimbs, which do not extend forward beyond tip of snout; from *P. masobe* by much smaller eyes and absence of a dorsal row of paired spines on the tail; from *P. fasciata*, *P. homalorhina*, *P. hordiesi*, *P. vahiny*, and *P. spelaea* by presence of spines on the original tail (versus absence); from *P. gracilis*, *P. homalorhina*, *P. kloki*, *P. maingoka*, *P. masobe*, *P. oviceps* (from its type locality Nosy Be), *P. picta*, *P. spelaea*, most *P. tanjaka*, and *P. vahiny* by the presence of prominent dorsal tubercles arranged in regular longitudinal rows (versus rather irregular rows of dorsal tubercles).

Within the *P. bastardi* clade, the species can easily be distinguished from *P. tanjaka* and *P. neglecta* by the absence of contact between the nostril and the rostral

scale (versus presence). It can be distinguished from *P. ibityensis* by larger maximum SVL (> 70 mm versus 61 mm). In comparison with *P. bastardi* sensu novo and *P. guibeae*, the new species can be distinguished by the presence of a very sharp and contrasting dark transverse pattern, evoking the shape of a thin curly-bracket ({), in the occipital region and delimiting the skull from the neck. Moreover, *Paroedura rennerae* sp. nov. is unambiguously larger in size than *P. guibeae* (adult SVL > 70 mm versus < 60 mm in *P. guibeae*), and its dorsal tubercles are more prominent. It also lacks striped fingers (versus striped in *P. guibeae*), and the light patch on its head lacks concave anterior edge and central vacuity in juveniles (versus both present in *P. bastardi*).

Description of the holotype. Adult female in very good condition, with the exception of the regenerated tail tip, which is amputated (ca. 10 mm missing). Head distinctly wider than neck, as wide as the body. Canthal ridges relatively well developed with a marked median depression. Ear opening is a vertical slit. Tail regenerated, nearly round (slightly flattened dorso-ventrally) in cross section in its proximal part; ventral pygal section of tail with a pair of poorly developed postcloacal sacs. Digits distinctly expanded at tips. Rostral scale rectangular, more than two times wider than tall and barely wider than mental. Nostrils separated from the rostral by prenasals. The two enlarged prenasals in contact with rostral and first supralabials, both separated by a single small granular scale. 12/12 (left/right) smooth supralabials, followed by two carinated tubercles above the mouth commissure. Eyes desiccated. Scales covering canthal ridges, loreal, temporal and periphery of the parietal region distinctly enlarged, spiny and tuberculate. Scales covering the dorsolateral side of neck and body heterogeneous, with enlarged, spiny, carinate and tuberculate scales regularly separated from each other by one (most often transversally) to three (most often longitudinally) rows of small, flat and juxtaposed scales or, along the vertebral line, by a single distinct row of smaller spiny tubercles. Seventeen longitudinal rows of tuberculate scales at midbody. Dorsal scales of forelimbs and hindlimbs mostly tuberculate and keeled, with a tetrahedral outline. Ventral scales of forelimbs distinctly smaller than surrounding ventral scales of the body. Three transverse rows at the base of the tail with six very spiny pygal scales per row. Ventrally, six rows of pygal scales squared and flat. Tail segments with irregular transverse row of spiny tubercles. Mental triangular, bordered posteriorly by a pair of elongated, irregular hexagonal postmentals. Each postmental in contact with six scales: other postmental, mental, first infralabial, one enlarged lateral gular, one smaller posterolateral gular, and one larger central gular. First three infralabials slightly larger (taller) than others. Gulars small, slightly granular. Ventrals of chest and abdomen flat and roundish. Proximal subdigitals in rows of mostly two. One pair of squarish terminal lamellae. Claws curving downwards between terminal pads of digits.

Measurements of the holotype (in mm): SVL = 73.6; TaL = 34.2 (tail regenerated and incomplete, distal tip of

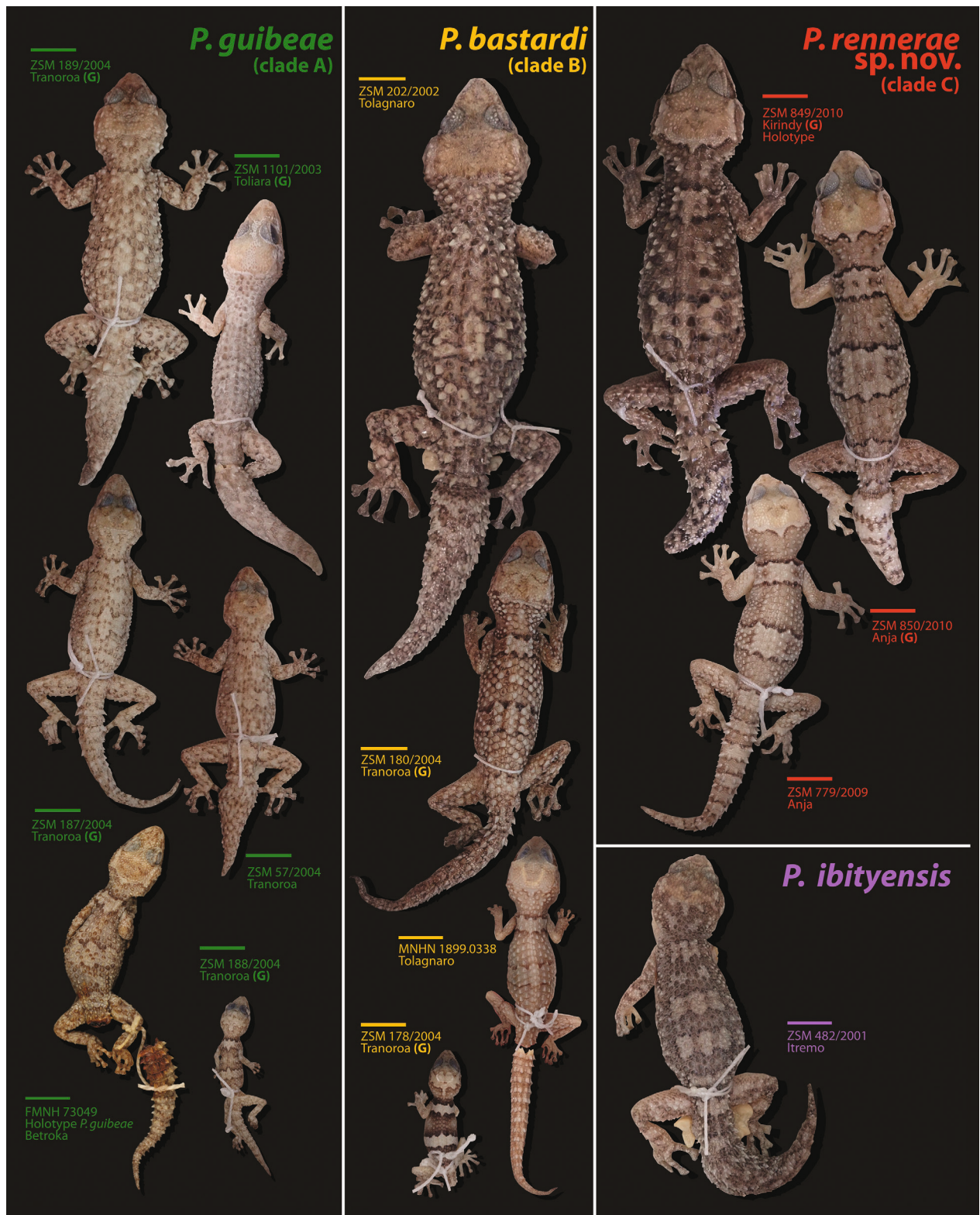


Figure 7. An overview of morphological diversity among the *P. bastardi* complex plus *P. ibityensis*. All specimens (adults, subadults and juveniles) are represented at the same scale (scale bar = 1 cm). Genotyped specimens are marked by the letter (G). Photo credit: FMNH 73049 ©Field Museum of Natural History. Created by Field Museum of Natural History, Amphibian and Reptile Collection and licensed under CC-BY-SA 4.0. All other pictures taken by AM.

ca. 10 mm missing); HL = 21.0; HW = 16.9; HH = 10.1; AGL = 32.4; distE = 2.7, ED = 5.3, EO = 2.7; HAL = 8.6; TIBL = 13.0; FoL = 11.5.

After nine years in alcohol (Fig. 9), head dorsally ochre colored with a pair of dark temporal bands, run-

ning from the eyes to contact each other in the nuchal region. The contrast between the ochre dorsal side of the head and the darker temporal/nuchal bands is amplified by a dark blackish curly-bracket shaped transverse stripe in the occipital region (Fig. 8). Area along the

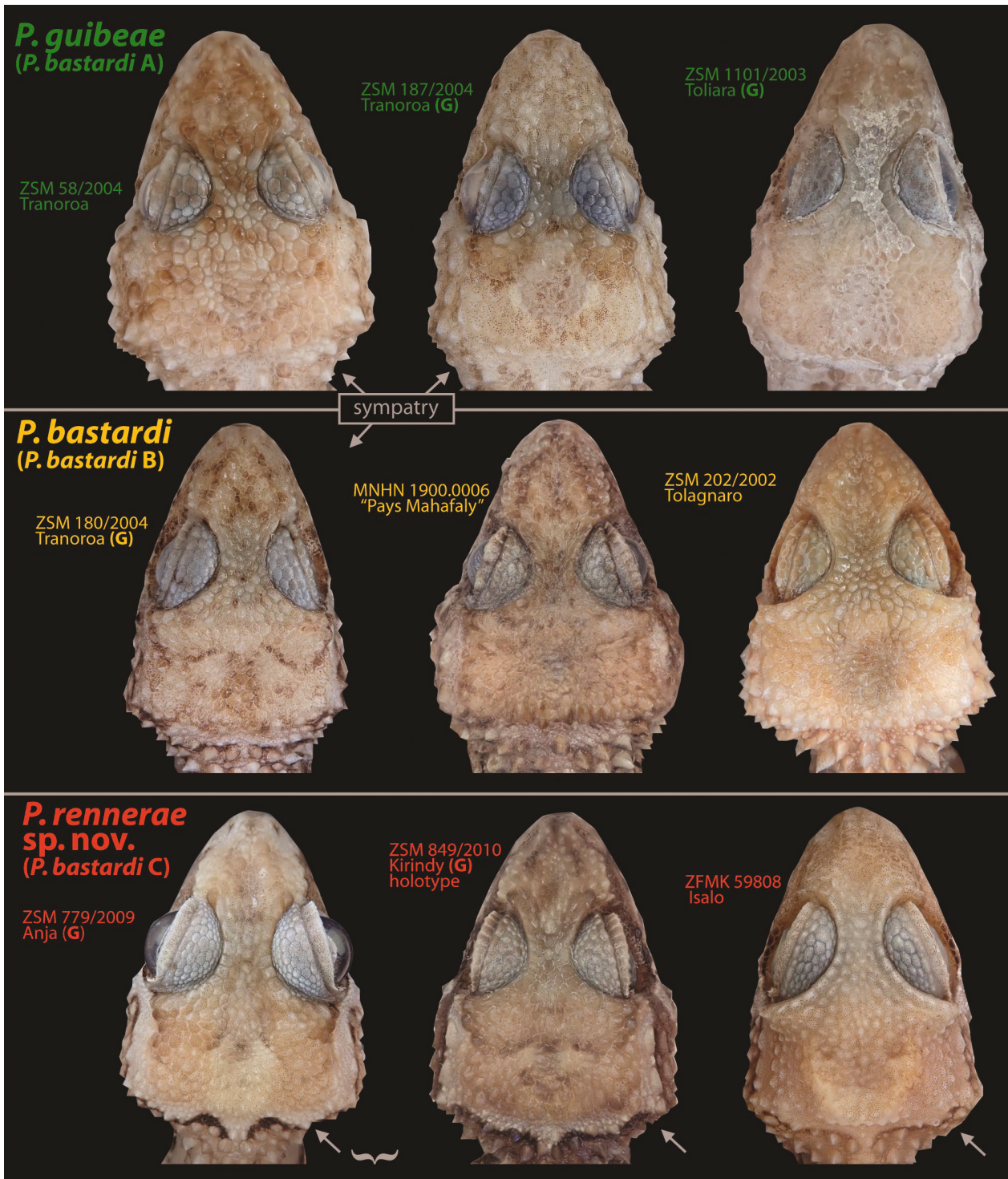


Figure 8. Details of the dorsal side of the head of the *P. bastardi* complex. Genotyped specimens are marked by the letter (G). Horizontal curly bracket ({) highlights the dark, contrasted and curved nuchal pattern evoking this symbol characterizing the specimens of *Paroedura rennerae* sp. nov. All pictures taken by AM.

upper lip alternating taupe-gray and cream. Body dorsally brown with three distinct lighter ochre (strongly contrasting thanks to very dark anterior and posterior borders) crossbands fading at the flanks: one transverse light crossband below forelimb insertion (width along the vertebral axis 6.1 mm), one distinctly broader light bow-tie-shaped crossband at midbody (width along the vertebral axis 9.6 mm), and one slightly less distinct band between the hindlimbs (6.3 mm). Dorsal surface-

es of forelimbs and hindlimbs slightly marbled with brown and ochre (hindlimbs not darker than forelimbs). Flank coloration lighter than dorsum, fading gradually towards the ventral surface. Ventral coloration (throat, chest, abdomen, ventral parts of forelimbs and hindlimbs) cream (very slightly pigmented on the throat and chest).

Coloration in life (Fig. 9). The coloration of the preserved specimen is very similar to that of the living in-

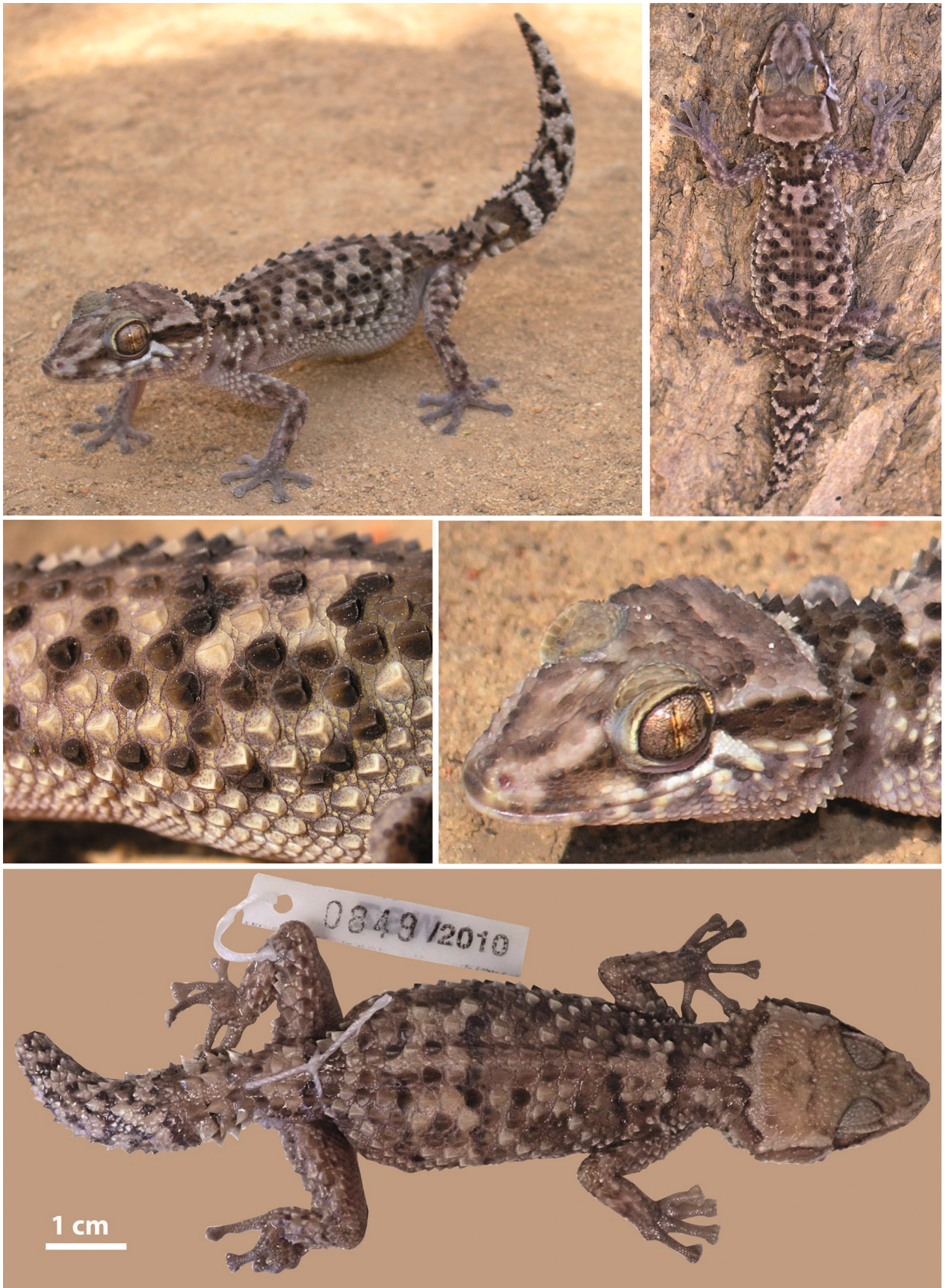


Figure 9. Holotype of *Paroedura rennerae* sp. nov. (ZSM 849/2010, from Kirindy CNFEREF). The four top photographs are of the living specimen, whereas the bottom picture shows the preserved specimen after nine years in 70% ethanol (pictures by AM).

dividual, although it is slightly duller (the contrasts are a little less strong and the colors a little less warm).

Variation. Both paratypes, from Anja, present a lighter and more contrasted color pattern, with sharper dark lines

Table 1. Phenotypic variation in *Paroedura rennerae* sp. nov. See Materials and Methods for abbreviations of measurements and scale counts.

Collection number	ZSM 849/2010	ZSM 779/2009	ZSM 850/2010	ZFMK 59808
Status	Holotype	Paratype	Paratype	none
Description	adult female	subadult	adult	juvenile
Locality	Kirindy	Anja	Anja	Isalo
Genotyped	yes	yes	yes	no
IO	5	5	4	5
SnoutS	c	s/i	s/i	c/s
SO (each sides)	5 (both sides)	4 (both sides)	5 (both sides)	4 (both sides)
Toe coloration	uniform	uniform	uniform	uniform
SVL (mm)	73.6	49.7	80.9	39.9
TL (mm)	N/A	42.5	N/A	36.3
HL (mm)	21.2	16.0	25.9	13.3
HW (mm)	17.1	12.6	17.3	10.1
HH (mm)	10.4	7.5	10.3	6.4
distE (mm)	2.7	2.0	2.8	1.7
AGL (mm)	32.2	18.5	32.7	16
ED (mm)	5.3	3.7	4.8	4
EO (mm)	2.7	1.9	3.3	1.7
HAL (mm)	8.6	6.7	8.9	5
TIBL (mm)	13.0	9.6	13.3	8.3

(anterior and posterior margin of the light dorsal cross bands and dark curly-brackets delimiting the occipital region) (Figs 7–8). The tail of ZSM 779/2009, which is not regenerated, has seven pairs of regularly alternating light brown and cream crossbands delimited by dark (brown) transverse stripes, whereas the tail of ZSM 850/2010 (regenerated) is cream with five thin transverse zig-zagging dark brown stripes (Fig. 7). The specimen ZFMK 59808, juvenile (but not neonate) with its original tail, is relatively similar in coloration to the paratype ZSM 779/2009, although slightly paler. In contrast with adults with a regenerated tail, younger specimens (ZSM 779/2009, subadult and ZFMK 59808, juvenile) present very regular rows of spiny tubercles all along the tail (around 20 rows). See also Table 1 for the variation in measurements.

Etymology. This new species, elegant and prickly, is dedicated to Susanne Renner, eminent botanist and evolutionary biologist, and Professor Emeritus of the University of Munich, in recognition of her substantial contributions to taxonomy and her invaluable collaboration in the framework of the “Taxon-omics” priority program of the German Research Foundation, DFG.

Habitat, habits, and distribution. *Paroedura rennerae* is reliably known from five localities, some of them relatively distant from each other, suggesting this species is widely distributed in the central/southern region of Madagascar. In the dry forest of Kirindy CNFEREF, specimens have been observed on vertical surfaces (tree trunks, wooden walls of the CNFEREF camp huts), around 1 to 2 m above the ground. Like other members of the *P. bastardi* species complex, it is quick to bite when handled. In Anja, several specimens have been collected

on granitic boulders. ZSM 779/2009 was found in a large cavity below two large granitic boulders, in a quite humid environment. In this cavity, ZSM 779/2009 and other individuals were found on the walls. In Isalo, specimens belonging to this species were found at two sites (Zahavola and Namazaha Valley). These individuals were found within the canyons of the sandstone Massif in shaded areas and in close proximity to a small cave or a small waterfall, again in quite humid microhabitats. Two additional 16S sequences confirm the presence of this species also in Marofandilia and Miandrivazo (GU129005 and GU128989, Aprea et al. 2013). All specimens have been observed at night or near dusk.

Discussion

Diversity, biogeography and species delimitation in the *Paroedura bastardi* clade

The genus *Paroedura* has seen a remarkable increase in the number of recognized species. Only nine species were recognized by Dixon and Kroll (1974), whereas Köhler et al. (2019) distinguished 22 species, and already pointed to the probable existence of additional species in the *P. bastardi* clade. By resurrecting *P. guibeae* and naming *P. rennerae*, the genus now contains 24 species, and we suspect that additional unnamed species still exist – for instance the enigmatic *P. bastardi* D identified herein.

As seems to be typical for many other reptiles in Madagascar, *Paroedura* contains several regional endemics

with moderately large distributions, as well as a handful of extremely range-restricted species. For instance, several *Paroedura* species specialized on karstic limestone often inhabit caves, and are restricted to particular limestone massifs (Glaw et al. 2018). The Ankarana Massif in northern Madagascar harbors microendemic gecko species of the genera *Paroedura* (i.e., *P. homalorhina*; Glaw et al. 2018), *Blaesodactylus* (*B. microtuberculatus*; Jono et al. 2015), *Geckolepis* (*G. megalepis*; Scherz et al. 2017), *Phelsuma* (*P. roesleri*; Glaw et al. 2010), and *Uroplatus* (*U. fetsy*; Ratsavina et al. 2019), and at least in the latter case, the closest relative of the microendemic species is more widespread. The *P. bastardi* clade also contains microendemic species (*P. neglecta* and *P. tanjaka*, only known from the Tsingy de Bemaraha limestone massif) and species spread over wider ranges in southern Madagascar (*P. bastardi*, *P. guibeae*, and *P. rennerae*), but a further example for microendemism in the genus might be *P. bastardi* D from Anja, whose status we could not reliably determine due to the lack of material. Anja Reserve is characterized by a specific habitat of large granitic boulders where range-restricted species of ground chameleons (*Brookesia brunoi*; Crottini et al. 2012) and geckos (*Phelsuma gouldi*; Crottini et al. 2011; *Paragehyra felicitae*; Crottini et al. 2014) occur. We recommend extended sampling in this area to clarify the status of *P. bastardi* D, and to identify possible additional microendemic species occurring at this site.

The improved knowledge on the taxonomy of the *P. bastardi* complex will, in the future, allow specifically targeting questions on possible ecological or behavioral specialization of the taxa involved. Especially in cases of sympatric occurrence, we assume that possibly, the taxa involved may prefer different substrates. We have found *P. bastardi* mostly on tree trunks and other vertical wooden surfaces, and the same is true for *P. rennerae* in Kirindy, but not in Anja, where at least ZSM 779/2009 was found on the walls of a cave-like large cavity. In Isalo, *P. rennerae* and *P. guibeae* occur syntopically at least at one site (Zahavola). However, while *P. rennerae* was found in quite humid microhabitats (and always inside the canyons), *P. guibeae* was mostly found on rock surfaces in open grasslands near canyon entrances.

Instances of sympatric occurrence of lineages may not only serve to understand their ecological specialization; they can also provide one of the most reliable lines of evidence to delineate species, and this has been applied both by Köhler et al. (2019) and in this study for the *Paroedura bastardi* complex. While numerous approaches to species delimitation use geographic sorting of mitochondrial haplotypes as argument for species distinctness (see Sites and Marshall 2004), we emphasize that sympatry can be one of the most powerful arguments for species distinctness, if used properly. The essential aspect of sympatry is that two lineages co-occurring at the same site at the same time while maintaining their genetic identity, in principle must be reproductively isolated. However, there are several caveats that need to be taken into account, and the *Paroedura* example serves to recapitulate these. (1) First, in highly mobile species or long-distance migrants,

conspecific individuals representing different geographic variants may regularly occur in sympatry outside of the breeding season, thus not representing evidence for reproductive isolation. Such situations however are extremely unlikely in less mobile, small-sized taxa, and thus can be excluded for geckos. (2) Secondly, exceptional events such as human translocation can bring specimens of different geographic variants into situations of immediate co-occurrence where genetic admixture will only become apparent after multiple generations. While human translocation is common in commensal geckos, it is unlikely to be a major factor in *Paroedura*, especially given that many of our collections were made in natural areas and a distinct phylogeographic structure was obvious in several species such as *P. guibeae*. (3) Sympatric variation in one marker alone is insufficient for sound conclusion. Different alleles of both nuclear and mitochondrial genes can co-exist in the same population, and especially in mitochondrial DNA, examples of fast divergence in geographic isolation, subsequent admixture and thus co-occurrence of substantially diverged haplotypes at the same site are common. In such cases, it is paramount to assess the variation in other, independent sets of characters (Pardial et al. 2010), which can be morphological, ecological, or behavioral, or other unlinked molecular markers such as nuclear gene sequences.

In the *P. bastardi* clade, there are at least two examples that will require future scrutiny: in *P. tanjaka*, three mitochondrial haplogroups of substantial divergence co-occur in the Tsingy de Bemaraha (Fig. 3; see also Köhler et al. 2019), and in *P. guibeae*, two haplogroups co-occur in the Isalo Massif (Fig. 3; treated as different candidate species Ca02 and Ca03 by Cocca et al. 2018). In these cases, we found no evidence for divergence in the nuclear genes studied, and had too limited material available for a thorough morphological comparison, and therefore treated the respective individuals as conspecifics (representing deep conspecific mitochondrial lineages sensu Vieites et al. 2009). (4) Lastly, it has to be considered that particularly closely related lineages in a state of incipient speciation may be connected by hybrid zones, and the width of these is informative about the species status of the taxa involved (e.g., Dufresnes et al. 2020). Across such hybrid zones, limited sampling from one site (i.e., few samples sequenced for few molecular markers) involves the risk – even if unlikely – to choose individuals where these markers show a concordant signal and thus suggest reproductive isolation. In the case of the *P. bastardi* clade, however, this situation is very unlikely, especially because in Tranoroa we could assess a strong concordance not only of unlinked molecular markers, but also of molecular with morphological differentiation.

To conclude, we advocate that sympatry of lineages without genetic admixture is one of the most immediate means to delimit species, even with limited sample size, if several other biological phenomena are appropriately considered and can be excluded. It is important to emphasize the need for concordance of various characters or unlinked markers; by no means should new species be based on co-occurrence of different, even strongly diver-

gent mitochondrial haplotypes alone. The probability of recovering by chance concordant differentiation among different unlinked markers, or between molecular markers and morphology, decreases drastically with increasing numbers of markers and sampled individuals, and we suggest that this could be taken into account by probabilistic approaches to species delimitation.

Funding

The Portuguese National Funds through FCT – Fundação para a Ciência e a Tecnologia – supported the Investigador FCT (IF) grant to AC (IF/00209/2014). This study would not have been possible without the support to AM and TB in the framework of the Taxon-Omics priority program of the Deutsche Forschungsgemeinschaft (SPP 1991 - RE 603/29-1).

Competing interests

The authors have declared that no competing interests exist.

Acknowledgments

We are grateful to the Malagasy institutions for research, collection and export permits. The numerous samples analyzed in this study have been assembled over many years with the help of many colleagues, of whom we would like to acknowledge especially Parfait Bora, Franco Andreone, Gonçalo M. Rosa, Vincenzo Mercurio, Fabio Mattioli, Devin Edmonds, Isabella Lau, D. James Harris, Iker A. Irisarri, Alexandra Lima, Solohery Rasamison, Emile Rajeriarison, Anicet, Haza, Aronina Rajaonarivo, Gennaro Aprea, Hildegard Enting, Kathrin Glaw, Marta Puente, Liliane Raharivoloniaina, Luris Rakotozafy, Roger Randrianiaina, R. Razafindraso, Meike Teschke, and David R. Vieites. We are furthermore grateful to Alan Resetar for the loan of specimens from the Field Museum of Natural History (FMNH), and to Josh Mata of the FMNH for providing high resolution pictures of the holotype of *P. guibae*. We are also indebted to Dennis Rödder and Morris Flecks for the loan of specimens from the ZFMK collection. We thank Meike Kondermann, Miriam Rabenow, and Kevin Oliphant for help with laboratory and analytical work. This work was carried out in the framework of collaboration accords among the authors' institutions and the Department of Animal Biology of the University of Antananarivo and the Ministry of the Environment of the Republic of Madagascar.

References

Aprea G, Andreone F, Fulgione D, Petraccioli A, Odierna G (2013) Chromosomal rearrangements occurred repeatedly and independently during species diversification in Malagasy geckos, genus *Paroedura*. African Zoology 48: 96–108. <https://doi.org/10.3377/004.048.0101>

Bruford MW, Hanotte O, Brookfield JFY, Burke T (1992) Single-locus and multilocus DNA fingerprinting. In: Hoelzel AR (Ed.) Molecu-

lar genetic analysis of populations: a practical approach. IRL Press, Oxford, pp. 225–270.

Chavent M, Kuentz V, Labenne A, Lique B, Saracco J (2017) PCAmix-data: Multivariate Analysis of Mixed Data. R package version 3.1. <https://CRAN.R-project.org/package=PCAmixdata>

Clement M, Posada D, Crandall KA (2000) TCS: a computer program to estimate gene genealogies. Molecular Ecology 9: 1657–1660. <https://doi.org/10.1046/j.1365-294x.2000.01020.x>

Cocca W, Rosa GM, Andreone F, Aprea G, Bergò PE, Mattioli F, Mercurio V, Randrianirina JE, Rosado D, Vences M, Crottini A (2018) The herpetofauna (Amphibia, Crocodylia, Squamata, Testudines) of the Isalo Massif, Southwest Madagascar: combining morphological, molecular and museum data. Salamandra 54: 178–200.

Crottini A, Gehring P-S, Glaw F, Harris DJ, Lima A, Vences M (2011) Deciphering the cryptic species diversity of dull-coloured day geckos *Phelsuma* (Squamata: Gekkonidae) from Madagascar, with description of a new species. Zootaxa 2982: 340–348. <https://doi.org/10.11646/zootaxa.2982.1.4>

Crottini A, Harris DJ, Miralles A, Glaw F, Jenkins RKB, Randrianantoandro JC, Bauer A, Vences M (2014) Morphology and molecules reveal two new species of the poorly studied gecko genus *Paragehyra* (Squamata: Gekkonidae) from Madagascar. Organisms, Diversity and Evolution 15: 175–198. <https://doi.org/10.1007/s13127-014-0191-5>

Crottini A, Miralles A, Glaw F, Harris DJ, Lima A, Vences M (2012) Description of a new pygmy chameleon (Chamaeleonidae: *Brookesia*) from central Madagascar. Zootaxa 3490: 63–74. <https://doi.org/10.11646/zootaxa.3490.1.5>

de Vienne DM, Giraud T, Martin OC (2007) A congruence index for testing topological similarity between trees. Bioinformatics 23(23): 3119–3124. <https://doi.org/10.1093/bioinformatics/btm500>

Dixon JR, Kroll JC (1974) Resurrection of the generic name *Paroedura* for the phyllodactyline geckos of Madagascar, and description of a new species. Copeia 1974(1): 24–30. <https://doi.org/10.2307/1443003>

Dray S, Dufour AB (2007) The ade4 package: Implementing the duality diagram for ecologists. Journal of Statistical Software 22(4): 1–20. <http://hdl.handle.net/10.18637/jss.v022.i04>

Dubois A (2007) Genitives of species and subspecies nomina derived from personal names should not be emended. Zootaxa 1550: 49–68. <https://doi.org/10.11646/zootaxa.1550.1.2>

Dufresnes C, Pribille M, Alard B, Gonçalves H, Amat F, Crochet PA, Dubey S, Perrin N, Fumagalli L, Vences M, Martínez-Solano I (2020) Integrating hybrid zone analyses in species delimitation: lessons from two anuran radiations of the Western Mediterranean. Heredity 124: 423–438. <https://doi.org/10.1038/s41437-020-0294-z>

Glaw F, Gehring PS, Köhler J, Franzen M, Vences M (2010) A new dwarf species of day gecko, genus *Phelsuma*, from the Ankarana pinnacle karst in northern Madagascar. Salamandra 46(2): 83–92.

Glaw F, Köhler J, Vences M (2018) Three new species of nocturnal geckos of the *Paroedura oviceps* clade from xeric environments of Madagascar (Squamata: Gekkonidae). Zootaxa 4433(2): 305–324. <https://doi.org/10.11646/zootaxa.4433.2.4>

Glaw F, Rösler H, Ineich I, Gehring PS, Köhler J, Vences M (2014) A new species of nocturnal gecko (*Paroedura*) from karstic limestone in northern Madagascar. Zoosystematics and Evolution 90: 249–259. <https://doi.org/10.3897/zse.90.8705>

Glaw F, Vences M (2007) A Field Guide to the Amphibians and Reptiles of Madagascar. 3rd edition. Vences and Glaw Verlag, Köln, 496 pp.

- Glaw F, Vences M, Schmidt K (2001) A new species of *Paroedura* Günther from northern Madagascar (Reptilia, Squamata, Gekkonidae). *Spixiana* 24: 249–256.
- Hara Y, Takeuchi M, Kageyama Y, Tatsumi K, Hibi M, Kiyonari H, Kuraku S (2018) Madagascar ground gecko genome analysis characterizes asymmetric fates of duplicated genes. *BMC Biology* 16: 40. <https://doi.org/10.1186/s12915-018-0509-4>
- Hawiltschek O, Glaw F (2013) The complex colonization history of nocturnal geckos (*Paroedura*) on the Comoros Archipelago. *Zoologica Scripta* 42: 135–150. <https://doi.org/10.1111/zsc.12001>
- International Commission on Zoological Nomenclature (1999) International Code of Zoological Nomenclature. Fourth edition. London: The International Trust for Zoological Nomenclature.
- Jackman TR, Bauer AM, Greenbaum E, Glaw F, Vences M (2008) Molecular phylogenetic relationships among species of the Malagasy-Comoran gecko genus *Paroedura* (Squamata: Gekkonidae). *Molecular Phylogenetics and Evolution* 46: 74–81. <https://doi.org/10.1016/j.ympev.2007.10.018>
- Jono T, Bauer AM, Brennan I, Mori A (2015) New species of *Blaesodactylus* (Squamata: Gekkonidae) from Tsingy karstic outcrops in Ankarana National Park, northern Madagascar. *Zootaxa* 3980(3): 406–416. <https://doi.org/10.11646/zootaxa.3980.3.4>
- Köhler J, Vences M, Scherz MD, Glaw F (2019) A new species of nocturnal gecko, genus *Paroedura*, from the karstic Tsingy de Bemaraha formation in western Madagascar. *Salamandra* 55(2): 73–81.
- Koubová M, Johnson Pokorná M, Rovatsos M, Farkačová K, Altmanová M, Kratochvíl L (2014) Sex determination in Madagascar geckos of the genus *Paroedura* (Squamata: Gekkonidae): are differentiated sex chromosomes indeed so evolutionary stable? *Chromosome Research* 22: 441–452. <https://doi.org/10.1007/s10577-014-9430-z>
- Kumar S, Stecher G, Tamura K (2016) MEGA7: Molecular Evolutionary Genetics Analysis Version 7.0 for Bigger Datasets. *Molecular Biology and Evolution* 33(7): 1870–1874. <https://doi.org/10.1093/molbev/msw054>
- Lanfear R, Frandsen PB, Wright AM, Senfeld T, Calcott B (2016) PartitionFinder 2: new methods for selecting partitioned models of evolution for molecular and morphological phylogenetic analyses. *Molecular Biology and Evolution* 34: 772–773. <https://doi.org/10.1093/molbev/msw260>
- Librado P, Rozas J (2009) DnaSP v5: A software for comprehensive analysis of DNA polymorphism data. *Bioinformatics* 25: 1451–1452. <https://doi.org/10.1093/bioinformatics/btp187>
- Michels JP, Bauer AM (2004) Some corrections to the scientific names of amphibians and reptiles. *Bonner Zoologische Beiträge* 52: 83–94.
- Mocquard F (1900) Diagnoses d'espèces nouvelles de reptiles de Madagascar. *Bulletin du Muséum national d'Histoire naturelle, Paris* 6(7): 345–348.
- Nagy ZT, Sonet G, Glaw F, Vences M (2012) First large-scale DNA barcoding assessment of reptiles in the biodiversity hotspot of Madagascar, based on newly designed COI primers. *PLoS ONE* 7: e34506. <https://doi.org/10.1371/journal.pone.0034506>
- Nussbaum RA, Raxworthy CJ (1994) A new rainforest gecko of the genus *Paroedura* Günther from Madagascar. *Herpetological Natural History* 2(1): 43–49.
- Nussbaum RA, Raxworthy CJ (2000) Systematic revision of the genus *Paroedura* Günther (Reptilia: Squamata: Gekkonidae), with description of five new species. *Miscellaneous Publications (Museum of Zoology, University of Michigan)* 189: 1–26.
- Padial JM, Miralles A, de la Riva I, Vences M (2010) The integrative future of taxonomy. *Frontiers in Zoology* 7: 16. <https://doi.org/10.1186/1742-9994-7-16>
- Ratsoavina FM, Scherz MD, Tolley KA, Raselimanana AP, Glaw F, Vences M (2019) A new species of *Uroplatus* (Gekkonidae) from Ankarana National Park, Madagascar, of remarkably high genetic divergence. *Zootaxa* 4683: 84–96. <https://doi.org/10.11646/zootaxa.4683.1.4>
- R Core Team (2018) R: A language and environment for statistical computing. R Foundation for Statistical Computing, Vienna, Austria. URL <https://www.R-project.org>
- Rösler H, Krüger J (1998) Eine neue Unterart von *Paroedura bastardi* (Mocquard, 1900) (Sauria: Gekkonidae) aus dem zentralen Hochland von Madagascar. *Sauria* 20(2): 37–46.
- Ronquist F, Teslenko M, van der Mark P, Ayres DL, Darling A, Höhna S, Larget B, Liu L, Suchard MA, Huelsenbeck JP (2012) MrBayes 3.2: Efficient Bayesian phylogenetic inference and model choice across a large model space. *Systematic Biology* 61: 539–542. <https://doi.org/10.1093/sysbio/sys029>
- RStudio Team (2016) RStudio: Integrated Development for R. RStudio, Inc., Boston, MA. URL: <http://www.rstudio.com>
- Scherz MD, Daza JD, Köhler J, Vences M, Glaw F (2017) Off the scale: a new species of fish-scale gecko (Squamata: Gekkonidae: *Geckelepis*) with exceptionally large scales. *PeerJ* 5: e2955. <http://doi.org/10.7717/peerj.e2955>
- Sites JW Jr, Marshall JC (2004) Operational criteria for delimiting species. *Annual Review of Ecology, Evolution and Systematics* 35: 199–227. <https://doi.org/10.1146/annurev.ecolsys.35.112202.130128>
- Stephens M, Smith NJ, Donnelly P (2001) A new statistical method for haplotype reconstruction from population data. *The American Journal of Human Genetics* 68: 978–989. <https://doi.org/10.1086/319501>
- Uetz P, Freed P, Hošek J (eds.) (2020) The Reptile Database, <http://www.reptile-database.org>, accessed November 6 Dec. 2020.
- Vieites DR, Wollenberg KC, Andreone F, Köhler J, Glaw F, Vences M (2009) Vast underestimation of Madagascar's biodiversity evidenced by an integrative amphibian inventory. *Proceedings of the National Academy of Sciences of the U.S.A.* 106: 8267–8272. <https://doi.org/10.1073/pnas.0810821106>

Supplementary material 1

Appendix 1

Authors: Aurélien Miralles, Teddy Bruy, Angelica Crotini, Andolalao Rakotoarison, Fanomezana M. Ratsoavina, Mark D. Scherz, Robin Schmidt, Jörn Köhler, Frank Glaw, Miguel Vences

Data type: various

Explanation note: List of specimen examined.

Copyright notice: This dataset is made available under the Open Database License (<http://opendatacommons.org/licenses/odbl/1.0>). The Open Database License (ODbL) is a license agreement intended to allow users to freely share, modify, and use this Dataset while maintaining this same freedom for others, provided that the original source and author(s) are credited.

Link: <https://doi.org/10.3897/vz.71.e59495.suppl1>

Supplementary material 2

Appendix 2

Authors: Aurélien Miralles, Teddy Bruy, Angelica Crotini, Andolalao Rakotoarison, Fanomezana M. Ratsoavina, Mark D. Scherz, Robin Schmidt, Jörn Köhler, Frank Glaw, Miguel Vences

Data type: various

Explanation note: Primers and PCR conditions used for amplification of the gene fragments used in this study.

Copyright notice: This dataset is made available under the Open Database License (<http://opendatacommons.org/licenses/odbl/1.0>). The Open Database License (ODbL) is a license agreement intended to allow users to freely share, modify, and use this Dataset while maintaining this same freedom for others, provided that the original source and author(s) are credited.

Link: <https://doi.org/10.3897/vz.71.e59495.suppl2>

Supplementary material 3

Appendix 3

Authors: Aurélien Miralles, Teddy Bruy, Angelica Crotini, Andolalao Rakotoarison, Fanomezana M. Ratsoavina, Mark D. Scherz, Robin Schmidt, Jörn Köhler, Frank Glaw, Miguel Vences

Data type: various

Explanation note: List of samples and specimens included in the molecular analyses with their respective localities, voucher field numbers, institutional catalogue number (when available) and GenBank accession numbers: (3A) molecular sampling designed for species delineation, (3B) molecular sampling designed for phylogenetic inference.

Copyright notice: This dataset is made available under the Open Database License (<http://opendatacommons.org/licenses/odbl/1.0>). The Open Database License (ODbL) is a license agreement intended to allow users to freely share, modify, and use this Dataset while maintaining this same freedom for others, provided that the original source and author(s) are credited.

Link: <https://doi.org/10.3897/vz.71.e59495.suppl3>

Supplementary material 4

Appendix 4

Authors: Aurélien Miralles, Teddy Bruy, Angelica Crotini, Andolalao Rakotoarison, Fanomezana M. Ratsoavina, Mark D. Scherz, Robin Schmidt, Jörn Köhler, Frank Glaw, Miguel Vences

Data type: various

Explanation note: List of haplotypes inferred by PHASE and used in the analyses of haplotype network: (A) CMOS haplotypes. (B) KIAA1239 haplotypes.

Copyright notice: This dataset is made available under the Open Database License (<http://opendatacommons.org/licenses/odbl/1.0>). The Open Database License (ODbL) is a license agreement intended to allow users to freely share, modify, and use this Dataset while maintaining this same freedom for others, provided that the original source and author(s) are credited.

Link: <https://doi.org/10.3897/vz.71.e59495.suppl4>

Supplementary material 5

Appendix 5

Authors: Aurélien Miralles, Teddy Bruy, Angelica Crotini, Andolalao Rakotoarison, Fanomezana M. Ratsoavina, Mark D. Scherz, Robin Schmidt, Jörn Köhler, Frank Glaw, Miguel Vences

Data type: various

Explanation note: Best-fit substitution models and partition calculated using Partition Finder.

Copyright notice: This dataset is made available under the Open Database License (<http://opendatacommons.org/licenses/odbl/1.0>). The Open Database License (ODbL) is a license agreement intended to allow users to freely share, modify, and use this Dataset while maintaining this same freedom for others, provided that the original source and author(s) are credited.

Link: <https://doi.org/10.3897/vz.71.e59495.suppl5>

Supplementary material 6

Appendix 6

Authors: Aurélien Miralles, Teddy Bruy, Angelica Crotini, Andolalao Rakotoarison, Fanomezana M. Ratsoaivina, Mark D. Scherz, Robin Schmidt, Jörn Köhler, Frank Glaw, Miguel Vences

Data type: various

Explanation note: Phenotypic variation in *Paroedura rennerae* sp. nov., *P. guibeae*, *P. bastardi*, and *P. ibityensis*.

Copyright notice: This dataset is made available under the Open Database License (<http://opendatacommons.org/licenses/odbl/1.0>). The Open Database License (ODbL) is a license agreement intended to allow users to freely share, modify, and use this Dataset while maintaining this same freedom for others, provided that the original source and author(s) are credited.

Link: <https://doi.org/10.3897/vz.71.e59495.suppl6>

Supplementary material 7

Appendix 7

Authors: Aurélien Miralles, Teddy Bruy, Angelica Crotini, Andolalao Rakotoarison, Fanomezana M. Ratsoaivina, Mark D. Scherz, Robin Schmidt, Jörn Köhler, Frank Glaw, Miguel Vences

Data type: various

Explanation note: Contributions of the variables to the first four axes (PCs) of the PCA on morphological variables.

Copyright notice: This dataset is made available under the Open Database License (<http://opendatacommons.org/licenses/odbl/1.0>). The Open Database License (ODbL) is a license agreement intended to allow users to freely share, modify, and use this Dataset while maintaining this same freedom for others, provided that the original source and author(s) are credited.

Link: <https://doi.org/10.3897/vz.71.e59495.suppl7>